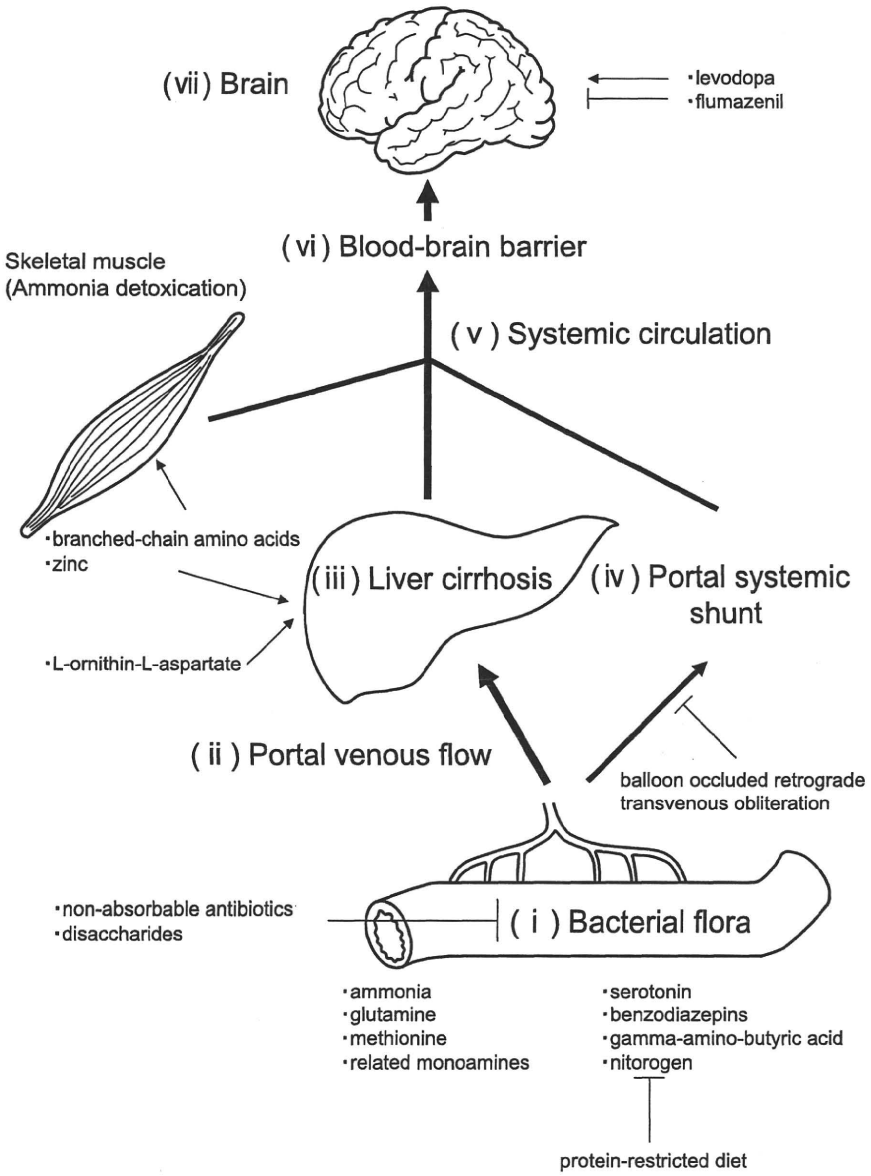

Figure 1 Pathophysiology of hepatic encephalopathy in liver cirrhosis, and action targets of therapeutic interventions. In patients with decompensated liver cirrhosis, (i) the endogenous neurotoxic substances are produced in the intestine by the bacterial flora, and (ii) are absorbed into the portal venous flow. They escape from catabolism by the liver, due both to (iii) the impaired function of the cirrhotic liver and also to (iv) the presence of portal systemic shunt. (v) These toxins then circulate at elevated concentrations in the systemic blood flow, (vi) reach the brain through the blood-brain barrier, and (vii) impair cerebral function leading to altered higher functions and consciousness. Therapeutic interventions either inhibit such pathophysiological pathways (⊥) or override (break down) the action of neurotoxins (vii). ←, levodopa; ⊢, flumazenil.

Table 1 Annual rate of occurrence of liver failure and its clinical symptoms in patients with liver cirrhosis, who have no past history of decompensation

	Annual rate	References
Hepatic failure (Total)	2–20%	10–14
Hepatic encephalopathy	8%	13
Ascites	7%	13
Edema	13%	13
Jaundice	9%	12

metabolic disorders such as hyperglycemia and hypoglycemia, and other organ failures, that is, the kidney, adrenal glands, and lung. In this context, it is important to note that the typical clinical sign of flapping tremor (asterixis) also appears in other disorders, such as hypoglycemia and renal insufficiency.

Supplemental clinical examinations for the diagnosis of hepatic encephalopathy are available, at first by psychometric tests such as the number connection test (NCT); this is particularly useful for the detection of minimal hepatic encephalopathy.[10,15,16] Medical imaging by computed tomography (CT)[17] and magnetic resonance

imaging (MRI)[18–22] usually show cerebral atrophy or, in acute type encephalopathy, cerebral edema. High-signal intensity of globus pallidus on MRI in liver cirrhosis is a famous sign, and is known to be brought about by manganese deposition. However, its specificity for hepatic encephalopathy is not yet definite, but rather seems to be due to portal systemic shunting.[18–21] Another MRI parameter, apparent diffusion coefficient (ADC) of water, has recently been reported as a reliable tool to quantify the grade of early hepatic encephalopathy in liver cirrhosis.[22] As an electrophysiological examination conventional electroencephalogram (EEG), shows slow waves with, sometimes, the appearance of triphasic wave. Somatosensory-evoked potential (SEP) is also useful.[23]

Epidemiology

Epidemiology of liver cirrhosis and hepatic encephalopathy

Epidemiology of liver cirrhosis depends particularly on the etiology, and shows a marked geographic difference worldwide, between Western, and Asian countries. While alcoholic consumption accounts for the majority in Western countries, hepatitis virus infection is the major cause of liver cirrhosis in the eastern hemisphere. In the latter region, hepatitis B virus (HBV) infection prevails on mainland Asia,[11] while two thirds of Japanese patients with cirrhosis are positive for hepatitis C virus (HCV).[24] Parasitic infection and intoxication with aflatoxin[25] in south-eastern Asia, and genetic disorders such as hemochromatosis[26] in Australia are also important causes of liver cirrhosis. The differences in the etiology of cirrhosis are significant with regard to the incidence of hepatocellular or cholangiocellular carcinoma, but no information is currently available on whether the development of hepatic encephalopathy depends on the cause of liver cirrhosis.

Incidence of hepatic encephalopathy

Studies on the incidence of liver failure in patients with liver cirrhosis, who have no past history of decompensation, are rare. Reliable longitudinal data in recently diagnosed with cirrhosis are available only in references #12, 20, 24, 25 and 26; the incidence ranges from 2% to 20%/year (Table 1). Among symptoms of decompensated cirrhosis, hepatic encephalopathy developed at an annual rate of 8% in one Japanese cohort.[13] Regarding the incidence of subclinical hepatic encephalopathy, a cross-sectional study of Child-Pugh grade A cirrhosis in China reported 40% had abnormal number connection test.[10]

Classification

Hepatic encephalopathy in liver cirrhosis is classified into two types; end-stage coma and chronic recurrent coma (Table 2).[1,13] These types are distinct in their prognosis, with poor survival rate in end-stage coma and favorable outcome for chronic recurrent encephalopathy (Table 2, Fig. 2). The precipitating factors in each type are listed in Table 2. The major cause of end-stage coma is massive gastrointestinal bleeding from ruptured esophageal varices or acute gastric mucosal lesion, while constipation/diarrhea, infection, and inappropriate use of diuretics are known to induce the chronic recurrent type. However, precipitating factors are unknown in approximately 30–40% of cases in both subtypes.

Table 2 Clinical subtypes of hepatic encephalopathy in liver cirrhosis (constructed based on the reference 13[13])

Subtype	End-stage coma	Chronic recurrent
Survival rate	23%	76%*
Precipitating factors	GI bleeding	Constipation/diarrhea
	Constipation/diarrhea	Infection
	Infection	Diuretics
	Renal failure	GI bleeding
		High protein diet
Duration (days)	13 (1–28)	3 (1–41)*
Maximum grade	IV	II*
Blood ammonia (ug/dL)	132	168
Prothrombin time (%)	43	54
Total bilirubin (mg/dL)	6	3*

Values are expressed as median.
*$P < 0.001$ as compared to end-stage coma.

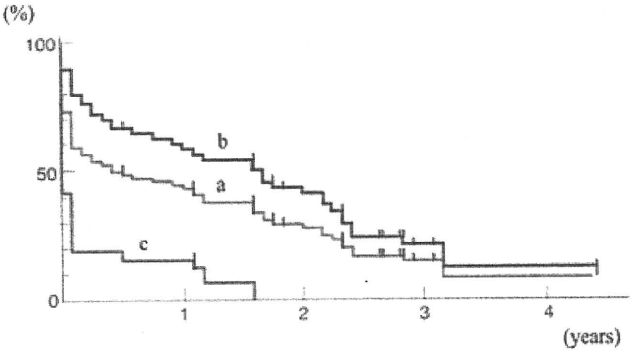

Figure 2 Survival rates of patients with liver cirrhosis from the initial episode of hepatic encephalopathy.[13] a. total, b, chronic recurrent type, and c, end-stage type hepatic encephalopathy.

Treatment

Candidate therapeutic modalities and interventions include protein- (or nitrogen-) restricted diet,[27–29] non-absorbable antibiotics,[30] oral disaccharides such as lactulose and lactitol,[31,32] disaccharide enema,[33] intravenous L-ornithine-L-aspartate (LOLA),[34] oral LOLA,[35] levodopa,[36] flumazenil,[37] intravenous or oral branched-chain amino acids (BCAA),[38–41] zinc supplementation,[42] portal-systemic shunt obliteration,[43] artificial liver support, and liver transplantation[44–46] (Fig. 1).

Among these therapeutics, first line treatment of hepatic encephalopathy in patients with liver cirrhosis has long been described as disaccharides, such as lactulose and lactitol.[1] However, recent studies including systematic reviews have questioned the effectiveness of this approach.[47–49] The most conservative statement in this regard at present is that treatment with lactulose/lactitol is effective at least against mild (including minimal) hepatic encephalopathy in cirrhosis,[50] but seems to require additional or alternative approaches for overt encephalopathy.[51–53]

In Eastern and Far East countries, therapeutic options are similar to those described above, but pronounced application of dietary restriction, antimicrobial agents, and disaccharides is noted. In particular, Asian researchers have been involved in the clinical development of portal systemic shunt obliteration, that is balloon-occluded retrograde transvenous obliteration (BRTO).[43] Other characteristic interventions in the eastern hemisphere include intensive use of branched chain amino acid formulas.[39,54] The latter approach is also becoming popular in these countries particularly to prevent the development of liver failure, as described later. In parallel, these studies elucidated that the patients with cirrhosis already have major nutritional challenges, that is protein-energy malnutrition,[55,56] and require adequate nutritional support.[27,57] Thus, we should emphasize that protein restriction is not recommended generally by current guidelines as a treatment of cirrhotic encephalopathy,[27,57] but applied only for exceptional cases who show severe nitrogen-intolerance.

Comprehensive therapy is usually employed for hepatic encephalopathy because it appears as only one of a broad range of symptoms in liver failure. Focusing on this particular problem, the therapeutic efficacy as given by the arousal rate is shown in Table 2. For the chronic recurrent type of encephalopathy, response rates range from 70% to 100%,[1,13] but treatment efficacy is quite poor in the end-stage type of encephalopathy. However, even in the chronic recurrent type, repeated episodes bring deterioration of the patients' liver function reserve and also their general condition of encephalopathy, contributing to a low survival rate, 30% at 3 years (Fig. 2),[13] and 14% at 5 years.[46] This rate is similar to those reported in the Western hemisphere.[58] Thus, broader application of liver transplantation seems to be absolutely essential for the improvement of such poor long-term survival.[46]

Prevention

Another option to improve the poor general outcome after hepatic encephalopathy is the prevention of this type of consciousness disorder in patients with liver cirrhosis. In this regard, interventional radiology, such as BRTO to shut down the portal systemic shunt,[43] and endoscopic intervention for risky esophageal varices, are promising approaches. In addition, advances have been made in this century by applying oral (enteral) BCAA formulas in both Western,[59] Asian[60] and also Far Eastern research (Fig. 3).[12] The mechanism of action is agreed to be improvement of protein-energy malnutrition and recovery of general condition in the decompensated patients.[12,56,57] Detoxification of ammonia by BCAA in skeletal muscle seems an attractive hypothesis to explain the mechanism of action of BCAA,[61] but further basic, as well as clinical, studies require high priority.

Conclusions

Hepatic encephalopathy is still a serious complication of liver cirrhosis. In spite of improved therapeutic options for each episode, long-term survival still remains low. Establishment of truly effective prevention modalities and broader application of liver transplantation will help rescue patients suffering from this complication of liver cirrhosis in the near future. In preparing this manuscript, we made strenuous efforts to highlight characteristics of cirrhotic encephalopathy in Asia. However, insufficient clinical and experimental description is available, unfortunately, as can be seen from the number of references from Asian countries only 17 among a total of 61 articles cited. Further studies from the eastern hemisphere are absolutely waited to establish global agreement with regard to the wider clinical aspects for cirrhotic encephalopathy.

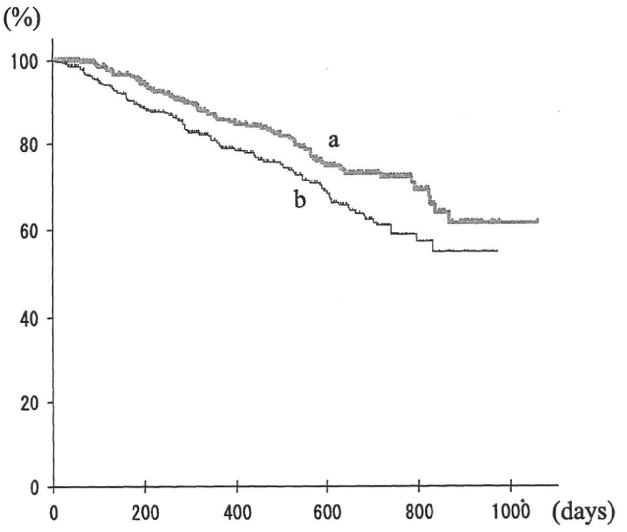

Figure 3 Effects of the oral supplementation with branched-chain amino acid granules on the event-free survival of patients with liver cirrhosis.[12] a, BCAA supplementation, b, control.

Acknowledgments

This work was supported in part by Grants-in-Aid for the Study Group for Intractable Liver Diseases and for the Study of Emerging and Reemerging Infectious Diseases from the Ministry of Health, Labor, and Welfare of Japan.

References

1 Sherlock S, Dooley J. Hepatic encephalopathy. In: Sherlock S, Dooley J, eds. *Diseases of the Liver and Biliary System*, 11th edn. Oxford: Blackwell Science, 2002; 87–102.
2 Plauth M, Roske A, Romaniuk P, Roth E, Ziebig R, Lochs H. Post-feeding hyperammonaemia in patients with transjugular intrahepatic portosystemic shunt and liver cirrhosis: role of small intestinal ammonia release and route of nutrient administration. *Gut* 2000; **46**: 849–55.
3 Mousseau DD, Butterworth RF. Current theories on the pathogenesis of hepatic encephalopathy. *Proc. Soc. Exp. Biol. Med.* 1994; **206**: 329–44.
4 Laubenberger J, Haussinger D, Bayer S, Gufler H, Hennig J, Langer M. Proton magnetic resonance spectroscopy of the brain in symptomatic and asymptomatic patients with liver cirrhosis. *Gastroenterology* 1997; **112**: 1610–16.
5 Mousseau DD, Baker GB, Butterworth RF. Increased density of catalytic sites and expression of brain monoamine oxidase A in humans with hepatic encephalopathy. *J. Neurochem.* 1997; **68**: 1200–8.
6 Mullen KD, Szauter KM, Kaminsky-Russ K. Endogenous

benzodiazepine activity in body fluids of patients with hepatic encephalopathy. *Lancet* 1990; **336**: 81–3.
7 Levy LJ, Leek J, Losowsky MS. Evidence for gamma-aminobutyric acid as the inhibitor of gamma-aminobutyric acid binding in the plasma of humans with liver disease and hepatic encephalopathy. *Clin. Sci. (Lond)* 1987; **73**: 531–4.
8 Ito Y, Nakamura T, Saito K *et al.* Pathophysiological role of intestinal flora in the Development of hepatic encephalopathy, with special reference to floral alterations induced by antimicrobial agents. *Microb. Ecol. Health Dis.* 1992; **5**: 1–13.
9 Ito Y, Moriwaki H, Muto Y, Kato N, Watanabe K, Ueno K. Effect of lactulose on short-chain fatty acids and lactate production and on the growth of faecal flora, with special reference to Clostridium difficile. *J. Med. Microbiol.* 1997; **46**: 80–4.
10 Li Y-Y, Nie Y-Q, Sha W-H *et al.* Prevalence of subclinical hepatic encephalopathy in cirrhotic patients in China. *World J. Gastroenterol.* 2004; **10**: 2397–401.
11 Yang SS, Wu CH, Chiang TR, Chen DS. Somatosensory evoked potentials in subclinical portosystemic encephalopathy: a comparison with psychometric tests. *Hepatology* 1998; **27**: 357–61.
12 Muto Y, Sato S, Watanabe A *et al.* Effects of oral branched-chain amino acid granules on event-free survival in patients with liver cirrhosis. *Clin. Gastroenterol. Hepatol.* 2005; **3**: 705–13.
13 Moriwaki H. Liver failure and hepatic encephalopathy. In: Sugimoto T, Yazaki Y, eds. *Textbook of Internal Medicine*, 9th edn. Tokyo: Asakura Shoten Co. Ltd., 2007; 933–6.
14 Lo KJ, Tong MJ, Chien MC *et al.* The natural course of hepatitis B surface antigen-positive chronic active hepatitis in Taiwan. *J. Infect. Dis.* 1982; **146**: 205–10.
15 Quero JC, Hartmann IJ, Meulstee J, Hop WC, Schalm SW. The diagnosis of subclinical hepatic encephalopathy in patients with cirrhosis using neuropsychological tests and automated electroencephalogram analysis. *Hepatology* 1996; **24**: 556–60.
16 Weissenborn K, Rückert N, Hecker H, Manns MP. The number connection tests A and B: interindividual variability and use for the assessment of early hepatic encephalopathy. *J. Hepatol.* 1998; **28**: 646–53.
17 Bernthal P, Hays A, Tarter RE, Van Thiel D, Lecky J, Hegedus A. Cerebral CT scan abnormalities in cholestatic and hepatocellular disease and their relationship to neuropsychologic test performance. *Hepatology* 1987; **7**: 107–14.
18 Rose C, Butterworth RF, Zayed J *et al.* Manganese deposition in basal ganglia structures results from both portal-systemic shunting and liver dysfunction. *Gastroenterology* 1999; **117**: 640–4.
19 Pomier-Layrargues G, Spahr L, Butterworth RF. Increased manganese concentrations in pallidum of cirrhotic patients. *Lancet* 1995; **345**: 735.
20 Nolte W, Wiltfang J, Schindler CG *et al.* Bright basal ganglia in T1-weighted magnetic resonance images are frequent in patients with portal vein thrombosis without liver cirrhosis and not suggestive of hepatic encephalopathy. *J. Hepatol.* 1998; **29**: 443–9.
21 Thuluvath PJ, Edwin D, Yue NC, deVilliers C, Hochman S, Klein A. Increased signals seen in globus pallidus in T1-weighted magnetic resonance imaging in cirrhotics are not suggestive of chronic hepatic encephalopathy. *Hepatology* 1995; **21**: 440–2.
22 Sugimoto R, Iwasa M, Maeda M *et al.* Value of the apparent diffusion coefficient for quantification of low-grade hepatic encephalopathy. *Am. J. Gastroenterol.* 2008; **103**: 1413–20.
23 Merican I, Guan R, Amarapuka D *et al.* Chronic hepatitis B virus infection in Asian countries. *J. Gastroenterol. Hepatol.* 2000; **15**: 1356–61.
24 Onji M. *Etiologies and Characteristics of Liver Cirrhosis in Japan 1998–2008.* Tokyo, Japan: Chugai Igaku Co. Ltd., 2008; 1–10.
25 El-Garem AA. Schistosomiasis. *Digestion* 1998; **59**: 589–605.
26 Merryweather-Clarke AT, Pointon JJ, Shearman JD, Robson KJ. Global prevalence of putative haemochromatosis mutations. *J. Med. Genet.* 1997; **34**: 275–8.
27 Plauth M, Cabre E, Riggio O *et al.* ESPEN guidelines on enteral nutrition: liver disease. *Clin. Nutr.* 2006; **25**: 285–94.
28 Mizock BA. Nutritional support in hepatic encephalopathy. *Nutrition* 1999; **15**: 220–8.
29 Cordoba J, Lopez-Hellin J, Planas M *et al.* Normal protein diet for episodic hepatic encephalopathy: results of a randomized study. *J. Hepatol.* 2004; **41**: 38–43.
30 Weber FL Jr, Fresard KM, Lally BR. Effects of lactulose and neomycin on urea metabolism in cirrhotic subjects. *Gastroenterology* 1982; **82**: 213–17.
31 Morgan MY, Hawley KE. Lactitol vs. lactulose in the treatment of acute hepatic encephalopathy in cirrhotic patients: a double-blind, randomized trial. *Hepatology* 1987; **7**: 1278–84.
32 Trovato GM, Catalano D, Carpinteri G, Runcio N, Mazzone O. Effects of lactitol [correction of lactilol] on hepatic encephalopathy and plasma amino-acid imbalance. *Recenti. Prog. Med.* 1995; **86**: 299–303.
33 Uribe M, Campollo O, Vargas F *et al.* Acidifying enemas (lactitol and lactose) *vs.* nonacidifying enemas (tap water) to treat acute portal-systemic encephalopathy: a double-blind, randomized clinical trial. *Hepatology* 1987; **7**: 639–43.
34 Kircheis G, Nilius R, Held C *et al.* Therapeutic efficacy of L-ornithine-L-aspartate infusions in patients with cirrhosis and hepatic encephalopathy: results of a placebo-controlled, double-blind study. *Hepatology* 1997; **25**: 1351–60.
35 Stauch S, Kircheis G, Adler G *et al.* Oral L-ornithine-L-aspartate therapy of chronic hepatic encephalopathy: results of a placebo-controlled double-blind study. *J. Hepatol.* 1998; **28**: 856–64.
36 Lunzer M, James IM, Weinman J, Sherlock S. Treatment of chronic hepatic encephalopathy with levodopa. *Gut* 1974; **15**: 555–61.
37 Barbaro G, Di Lorenzo G, Soldini M *et al.* Flumazenil for hepatic encephalopathy grade III and IVa in patients with cirrhosis: an Italian multicenter double-blind, placebo-controlled, cross-over study. *Hepatology* 1998; **28**: 374–8.
38 Morgan MY. Branched chain amino acids in the management of chronic liver disease. Facts and fantasies. *J. Hepatol.* 1990; **11**: 133–41.
39 Suzuki K, Kato A, Iwai M. Branched-chain amino acid treatment in patients with liver cirrhosis. *Hepatol. Res.* 2004; **30S**: 25–9.
40 Fabbri A, Magrini N, Bianchi G, Zoli M, Marchesini G. Overview of randomized clinical trials of oral branched-chain amino acid treatment in chronic hepatic encephalopathy. *JPEN J .Parenter. Enteral. Nutr.* 1996; **20**: 159–64.
41 Calvey H, Davis M, Williams R. Controlled trial of nutritional supplementation, with and without branched chain amino acid enrichment, in treatment of acute alcoholic hepatitis. *J. Hepatol.* 1985; **1**: 141–51.
42 Marchesini G, Fabbri A, Bianchi G, Brizi M, Zoli M. Zinc supplementation and amino acid-nitrogen metabolism in patients with advanced cirrhosis. *Hepatology* 1996; **23**: 1084–92.
43 Kawanaka H, Ohta M, Hashizume M *et al.* Portosystemic encephalopathy treated with balloon-occluded retrograde transvenous obliteration. *Am. J. Gastroenterol.* 1995; **90**: 508–10.
44 Parkes JD, Murray-Lyon IM, Williams R. Neuropsychiatric and electro-encephalographic changes after transplantation of the liver. *Q. J. Med.* 1970; **39**: 515.
45 Powell EE, Pender MP, Chalk JB *et al.* Improvement in chronic hepatocerebral degeneration following liver transplantation. *Gastroenterology* 1990; **98**: 1079–82.
46 de Jonah FE, Janssen HL, de Man RA *et al.* Survival and prognostic

indicators in hepatitis B surface antigen-positive cirrhosis of the liver. *Gastroenterology* 1992; **103**: 1692–4.
47 Als-Nielsen B, Gluud LL, Gluud C. Nonabsorbable disaccharides for hepatic encephalopathy. *Cochrane Database Syst. Rev.* 2004: 1–65.
48 Als-Nielsen B, Gluud LL, Gluud C. Non-absorbable disaccharides for hepatic encephalopathy: systematic review of randomised trials. *BMJ* 2004; **328**: 1046.
49 Shawcross D, Jalan R. Dispelling myths in the treatment of hepatic encephalopathy. *Lancet* 2005; **365**: 431–3.
50 Prasad S, Dhiman RK, Duseja A, Chawla YK, Sharma A, Agarwal R. Lactulose improves cognitive functions and health-related quality of life in patients with cirrhosis who have minimal hepatic encephalopathy. *Hepatology* 2007; **45**: 549–59.
51 Larsen FS, Wendon J. Alternative pathway therapy for hyperammonemia in liver failure. *Hepatology* 2009; **50**: 3–5.
52 Davies NA, Wright G, Ytrebø LM *et al.* L-ornithine and phenylacetate synergistically produce sustained reduction in ammonia and brain water in cirrhotic rats. *Hepatology* 2009; **50**: 155–64.
53 Ytrebø LM, Kristiansen RG, Maehre H *et al.* L-ornithine phenylacetate attenuates increased arterial and extracellular brain ammonia and prevents intracranial hypertension in pigs with acute liver failure. *Hepatology* 2009; **50**: 165–74.
54 Iwasa M, Matsumura K, Watanabe Y *et al.* Improvement of regional cerebral blood flow after treatment with branched-chain amino acid solutions in patients with cirrhosis. *Eur. J. Gastroenterol. Hepatol.* 2003; **15**: 733–7.
55 Alberino F, Gatta A, Amodio P *et al.* Nutrition and survival in patients with liver cirrhosis. *Nutrition* 2001; **17**: 445–50.
56 Tajika M, Kato M, Mohri H *et al.* Prognostic value of energy metabolism in patients with viral liver cirrhosis. *Nutrition* 2002; **18**: 229–34.
57 ASPEN Board of Directors and the Clinical Guidelines Task Force. Guidelines for the use of parenteral and enteral nutrition in adult and pediatric patients. *J. Parenter. Enteral. Nutr.* 2002; **26** (Suppl.): 73–5.
58 Bustamante J, Rimola A, Ventura PJ *et al.* Prognostic significance of hepatic encephalopathy in patients with cirrhosis. *J. Hepatol.* 1999; **30**: 890–5.
59 Marchesini G, Bianchi G, Merli M *et al.* Italian BCAA Study Group. Nutritional supplementation with branched-chain amino acids in advanced cirrhosis: a double-blind, randomized trial. *Gastroenterology* 2003; **124**: 1792–801.
60 Poon RT, Yu WC, Fan ST, Wong J. Long-term oral branched chain amino acids in patients undergoing chemoembolization for hepatocellular carcinoma: a randomized trial. *Aliment. Pharmacol. Ther.* 2004; **19**: 779–88.
61 Hayashi M, Ohnishi H, Kawade Y, Muto Y, Takahashi Y. Augmented utilization of branched-chain amino acids by skeletal muscle in decompensated liver cirrhosis in special relation to ammonia detoxication. *Gastroenterol. Jpn.* 1981; **16**: 64–70.

Ability of IDO To Attenuate Liver Injury in α-Galactosylceramide–Induced Hepatitis Model

Hiroyasu Ito,* Masato Hoshi,* Hirofumi Ohtaki,* Ayako Taguchi,† Kazuki Ando,*,‡ Tetsuya Ishikawa,§ Yosuke Osawa,* Akira Hara,† Hisataka Moriwaki,¶ Kuniaki Saito,‖ and Mitsuru Seishima*

IDO converts tryptophan to L-kynurenine, and it is noted as a relevant molecule in promoting tolerance and suppressing adaptive immunity. In this study, we examined the effect of IDO in α-galactosylceramide (α-GalCer)–induced hepatitis. The increase in IDO expression in the liver of wild-type (WT) mice administered α-GalCer was confirmed by real-time PCR, Western blotting, and IDO immunohistochemical analysis. The serum alanine aminotransferase levels in IDO-knockout (KO) mice after α-GalCer injection significantly increased compared with those in WT mice. 1-Methyl-D-tryptophan also exacerbated liver injury in this murine hepatitis model. In α-GalCer–induced hepatitis models, TNF-α is critical in the development of liver injury. The mRNA expression and protein level of TNF-α in the liver from IDO-KO mice were more enhanced compared with those in WT mice. The phenotypes of intrahepatic lymphocytes from WT mice and IDO-KO mice treated with α-GalCer were analyzed by flow cytometry, and the numbers of $CD49b^+$ and $CD11b^+$ cells were found to have increased in IDO-KO mice. Moreover, as a result of the increase in the number of NK cells and macrophages in the liver of IDO-KO mice injected with α-GalCer, TNF-α secretion in these mice was greater than that in WT mice. Deficiency of IDO exacerbated liver injury in α-GalCer–induced hepatitis. IDO induced by proinflammatory cytokines may decrease the number of TNF-α–producing immune cells in the liver. Thus, IDO may suppress overactive immune response in the α-GalCer–induced hepatitis model. *The Journal of Immunology*, 2010, 185: 4554–4560.

Indoleamine 2,3-dioxygenase has been identified as an enzyme that has powerful immunomodulatory effects, resulting from its enzymatic activity, which leads to catabolism of the essential amino acid L-tryptophan (L-Trp) to L-kynurenine (L-Kyn) (1, 2). This enzyme is expressed in epithelial, macrophage, and dendritic cells induced by proinflammatory cytokines, including type I and type II IFN (3, 4). The binding of CTLA-4 with CD80/CD86 on the membrane of dendritic cells also stimulates IDO transcriptional expression and activity (5, 6). Furthermore, metabolites of the L-Kyn pathway have been shown to act as immunoregulatory molecules that have immunosuppressive effects in the tissue microenvironment (7). IDO and the L-Trp pathway play critical roles in the generation of immune tolerance against foreign Ags in tissue microenvironments. Recently, we demonstrated that IDO expression on hepatocytes is increased in liver injury caused by hepatitis B virus-specific CTL in hepatitis B virus transgenic mice (8). Furthermore, it has been reported that IDO expressions in the liver and serum L-Kyn/L-Trp ratios in patients with chronic hepatitis C were increased and that this upregulation of IDO was caused by the IFN-γ produced by hepatitis C virus-activated T cells in the liver (9). As shown above, IDO expression is significantly enhanced during liver injury. We therefore established two hypotheses on the role of IDO: 1) IDO directly or indirectly brings about the progression of liver injury; and 2) IDO production is enhanced as a protective mechanism in liver injury. However, the actual role of IDO in liver injury remains unknown.

Several reports have demonstrated that α-galactosylceramide (α-GalCer), a specific ligand for invariant Vα14 NKT cells, induces liver injury (10–12). α-GalCer is hepatotoxic since the administration of α-GalCer in mice results in the activation and apoptosis of hepatic Vα14 NKT cells via activation-induced cell death and associated liver damage. Furthermore, the hepatotoxic effect of α-GalCer was found to be mediated by TNF-α produced by activated hepatic Vα14 NKT cells (12). In fact, it was proposed that TNF-α increases FasL expression on Vα14 NKT cells, and that these cells in turn promote liver damage by interacting with Fas-expressing hepatocytes (12). It is noteworthy that liver injury induced by α-GalCer is thought to potentially mimic some aspects of autoimmune hepatitis. The liver appears to be particularly susceptible to injury as a result of increased immune responses, mainly mediated by T lymphocytes and/or emerging autoantibodies. On viral infection of hepatocytes, the cytopathic effect of the virus per se is only moderate; instead, liver damage is caused by cellular immune responses to infected cells. Thus, the host immune system is related to the initiation and progression of liver injury in several liver injury models, and it is very important to determine the role of IDO and its powerful immunomodulatory effects during hepatic injury.

In this study, we examined the effect of IDO on α-GalCer–induced liver injury in mice and demonstrated that liver injury was exacerbated in IDO-deficient mice.

*Department of Informative Clinical Medicine, †Department of Tumor Pathology, and ¶First Department of Internal Medicine, Gifu University Graduate School of Medicine, Gifu; ‡Goto Clinic, Ogaki; §Cancer Immunotherapy Center, Nagoya Kyoritsu Hospital, Nagoya; and ‖Human Health Science, Graduate School of Medicine and Faculty of Medicine, Kyoto University, Kyoto, Japan

Received for publication December 28, 2009. Accepted for publication August 9, 2010.

Address correspondence and reprint requests to Dr. Hiroyasu Ito, Department of Informative Clinical Medicine, Gifu University Graduate School of Medicine, 1-1 Yanagido, Gifu 501-1194, Japan. E-mail address: hito@gifu-u.ac.jp

Abbreviations used in this paper: ALT, alanine aminotransferase; α-GalCer, α-galactosylceramide; IHL, intrahepatic lymphocyte; KC, keratinocyte chemoattractant; KO, knockout; L-Kyn, L-kynurenine; L-Trp, L-tryptophan; MNC, mononuclear cell; 1-MT, 1-methyl-D-tryptophan; WT, wild-type.

www.jimmunol.org/cgi/doi/10.4049/jimmunol.0904173

Materials and Methods

Mice

Male C57BL/6J wild-type (WT) mice (age, 8–10 wk; weight, 25–30 g) were obtained from Japan SLC (Shizuoka, Japan). IDO-knockout (KO) mice with a C57BL/6J background were obtained from The Jackson Laboratory (Bar Harbor, ME). All procedures were conducted in accordance with the National Institutes of Health Guide for the Care and Use of Laboratory Animals, and with the guidelines for the care and use of animals established by the Animal Care and Use Committee of Gifu University.

Animal treatment

α-GalCer was obtained from Funakoshi (Tokyo, Japan) and stored as a 200 μg/ml stock solution in vehicle (0.5% w/v polysorbate-20); it was then diluted in pyrogen-free saline to obtain the indicated dose directly before i.v. injection of a total volume of 200 μl/mouse. Hepatocellular injury was monitored biochemically through measurement of serum alanine aminotransferase (ALT) activity. At appropriate time points, mice were killed by cervical dislocation, and necropsy was performed. Tissue samples were fixed in 10% formalin, embedded in paraffin, and sectioned; the sections were then stained with H&E.

Immunohistochemical analysis

Tissues were fixed in 10% formalin in PBS overnight. Specimens were then embedded in paraffin. Sections that were 4 μm thick were used for H&E staining and immunohistochemical analysis for IDO as described previously (13). For the immunohistochemical analysis, the deparaffinized sections were heated in 0.1 M citrate buffer (pH 6.0), using the Pascal heat-induced target retrieval system (Dako, Carpinteria, CA). Nonspecific Ab binding sites were blocked in PBS (pH 7.4) containing 2% BSA (Wako Pure Chemical Industries, Osaka, Japan) for 60 min. The sections were then incubated with rabbit anti-IDO polyclonal Ab (anti-mouse IDO Ab was generated by the peptide H-CMKPSKKKPTDGDKS-OH) diluted 1/100 in 2% BSA/PBS and incubated overnight at 4°C. The IDO protein was shown by using a labeled streptavidin-biotin kit (Dako Japan, Kyoto, Japan) containing biotinylated Ab and peroxidase-labeled streptavidin. The peroxidase binding sites were detected by staining with 3,3′-diaminobenzidine. Finally, counterstaining was performed using Mayer's hematoxylin.

Determination of L-Kyn concentrations

Plasma from the mice was mixed with 3 volumes of 3% perchloric acid. After centrifugation, the concentrations of L-Kyn in the supernatants were measured using HPLC with a 5-mm octyldecylsilane column (150 × 2.1 mm; Eicom, Kyoto, Japan) and a spectrophotometric detector or a fluorescence spectrometric detector as described previously (13). UV signals were monitored at 355 nm for L-Kyn. The mobile phase consisted of 2.5% acetonitrile in 0.1 M sodium acetate (pH 3.9) and was filtered through a 0.45-μm-pore HA-type filter obtained from Millipore (Bedford, MA). The flow rate was maintained at 0.75 ml/min throughout the chromatographic run.

Analysis of liver transaminase

Hepatocyte damage was assessed at the indicated time points after α-GalCer injection through measurement of plasma ALT activities using an automated clinical analyzer (BM2250; JEOL, Tokyo, Japan).

Hepatic mononuclear cell preparation and flow cytometric analysis

Hepatic mononuclear cells (MNCs) were isolated and purified as previously described (14). Briefly, the excised liver was cut into small pieces with scissors, pressed through a 200-gauge stainless mesh, and suspended in PBS. Lymphocytes were separated from parenchymal hepatocytes and hepatocyte nuclei by Ficoll-Conray (IBL, Gunma, Japan) and washed twice in ice-cold medium. Cell viability and cell numbers were assessed by trypan blue exclusion. For flow cytometry, 2×10^5 liver MNCs were stained using a standard protocol. The following Abs were used: FITC-labeled hamster anti-mouse CD3ε mAb (clone 145-2c11), FITC-labeled rat anti-mouse CD4 mAb (clone RM4-5), FITC-labeled rat anti-mouse Gr-1 mAb (clone RB6-8C5), PE-labeled rat anti-mouse CD49b mAb (clone DX5), PE-labeled rat anti-mouse CD8a mAb (clone 53-6.7), and PE-labeled rat anti-mouse CD11b mAb (clone M1/70) (all from eBioscience, San Diego, CA). Samples were acquired on a FACStar flow cytometer, and data analysis was performed using CellQuest software (BD Biosciences, San Jose, CA).

Isolation of mouse hepatocytes

The abdomen of a sacrificed mouse was opened and a needle was inserted into the vena cava. The portal vein was punctured. The liver was perfused with PBS and liver perfusion medium (Invitrogen Life Technologies, Carlsbad, CA). To obtain nonparenchymal cell populations, the liver was perfused with liver digestion medium (Invitrogen Life Technologies), removed, and gently pressed through a mesh. Nonparenchymal cell were separated from parenchymal hepatocytes by centrifugation at 50 × *g* for 5 min. The purified cell population obtained in the final cell pellet was composed of ≥96% hepatocytes as previously reported (15).

Real-time PCR

Total RNA was isolated and transcribed into cDNA with an RNeasy Mini kit (Qiagen, Hilden, Germany) and High-Capacity cDNA Reverse Transcription kits (Applied Biosystems, Foster City, CA). The resulting cDNA was used as a template for real-time PCR along with primer/probe sets for IDO, TNF-α, IL-2, IL-4, IL-6, IL-10, IFN-γ, MCP-1, MIP-2, keratinocyte chemoattractant (KC), and TGF-β (TaqMan Gene Expression Assays; Applied Biosystems) and 2× TaqMan Universal PCR Master Mix (Applied Biosystems) according to the manufacturer's recommendations. The primer/probe sets for 18S were used as internal controls in the reactions (Applied Biosystems). Real-time PCR data were analyzed using sequence detector software (Applied Biosystems).

Western blot analysis

Protein (20 μg) from the cell lysate was subjected to SDS-PAGE and transferred to nitrocellulose membranes. After blocking nonspecific reactions with 5% skim milk, the membrane was incubated with anti-IDO and anti-GAPDH Abs for 60 min at room temperature and subsequently incubated with peroxidase-labeled anti-mouse or -rabbit IgG Ab for 60 min at room temperature. Immunoreactive protein bands were visualized with ECL Plus (GE Healthcare, Buckinghamshire, U.K.).

Cytokine and chemokine detection by ELISA

The concentrations of circulating TNF-α, IL-6, MIP-2, and KC in the sera were determined by an ELISA kit (R&D Systems, Minneapolis, MN), according to the manufacturer's instructions. The experimental results are expressed as the mean of triplicates (±SD) of three independent experiments.

Intracellular cytokine staining

For intracellular staining, hepatic MNCs from the mice that were administered α-GalCer were incubated for 4 h with brefeldin A (10 μg/ml). Then these cells were fixed, permeabilized with the Cytofix/Cytoperm buffer (BD Pharmingen, San Diego, CA), and stained with FITC-conjugated anti-mouse TNF-α (clone MP6-XT22; eBioscience). Samples were acquired on a FACStar flow cytometer, and data analysis was conducted using the CellQuest software (BD Biosciences).

Statistical analysis

Values are expressed as means (SEM). Differences between the experimental and control groups were analyzed by the Kruskal-Wallis test followed by the Scheffé *F* test. Significance was established at $p < 0.05$.

Results

Upregulation of IDO expression and activity in the liver after α-GalCer injection

We studied the increase in IDO in the liver as a result of α-GalCer treatment. As shown in Fig. 1*A*, to assess the changes in IDO activity in the WT and IDO-KO mice treated with α-GalCer, we first investigated the time course of changes in the serum L-Kyn concentration. The serum L-Kyn levels in WT mice were significantly increased at least as early as 20 h following α-GalCer (2 μg/mouse) injection compared with those in IDO-KO mice, and this increase in serum L-Kyn levels persisted on day 7 after α-GalCer injection. We next examined both IDO mRNA expression and IDO protein levels in the liver of WT and IDO-KO mice administered α-GalCer (Fig. 1*B–D*). IDO mRNA expression in the liver of WT mice was significantly increased at 24 h after α-GalCer injection. Western blot analysis and immunohistochemical examination revealed that the IDO protein levels in the livers from WT mice were upregulated

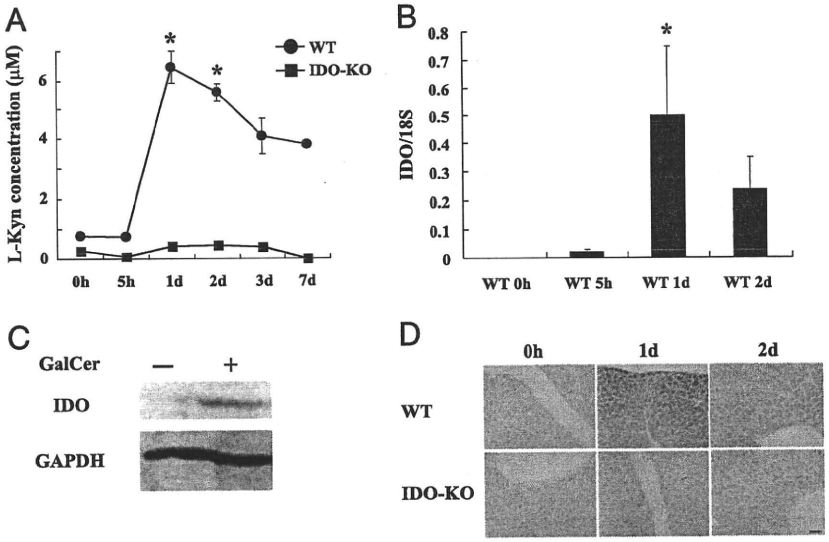

FIGURE 1. Upregulation of IDO expression and activity in the liver after α-GalCer injection. *A*, L-Kyn concentrations in serum determined by performing the HPLC method on WT and IDO-KO mice treated with α-GalCer. Each value is represented by the mean (SEM) of three mice. $*p < 0.05$. *B*, The relative expression levels of IDO mRNA in the livers of WT mice administered α-GalCer were measured using quantitative real-time PCR. The results were normalized by the expression of 18S mRNA. Each value is represented by the mean (SEM) of three mice. $*p < 0.05$. *C*, Expression of IDO protein in the livers of WT mice 1 d after treatment with α-GalCer was examined by Western blot analysis and was determined using the GAPDH protein. Data are representative of at least three independent experiments with similar results. *D*, Immunohistochemical analysis of IDO in the liver of WT and IDO-KO mice after α-GalCer injection. IDO protein was stained by using a labeled streptavidin-biotin kit containing biotinylated Ab and peroxidase-labeled streptavidin. The peroxidase binding sites were detected by staining with 3,39-diaminobenzidine. Scale bar, 25 μm. Original magnification ×200. Data are representative of at least three independent experiments with similar results.

after α-GalCer injection. This increase in IDO expression was observed in hepatocytes in particular.

Induction of liver injury by α-GalCer in WT mice and IDO-KO mice

To determine whether IDO plays a critical role in α-GalCer–induced liver injury, IDO-KO mice and WT mice were i.v. injected with α-GalCer (2 μg/mouse). Serum ALT activity started increasing at 12 h, reached a peak at 1 d, and returned to normal at 5 d after injection in WT mice (Fig. 2*A*). Surprisingly, serum ALT activity in IDO-KO mice significantly increased at 1 and 2 d after the injection compared with the activity in WT mice. To examine histological changes in the liver in the presence or absence of IDO after α-GalCer injection, we subjected liver tissues to H&E staining. As shown in Fig. 2*B*, livers from both WT and IDO-KO mice were mostly histologically normal except for a few very small and widely scattered necroinflammatory foci consisting of lymphomononuclear cells and apoptotic hepatocytes 1 d after α-GalCer injection. At 2 d after α-GalCer injection, the necroinflammatory foci in the livers of IDO-KO mice became larger and more abundant compared with those in WT mice, consisting of a mixed population of lymphomononuclear cells and apoptotic hepatocytes that often displayed granulomatous features in the hepatic parenchyma.

α-GalCer–induced TNF-α production in WT and IDO-KO mice

It was previously reported that neutralization of TNF-α significantly reduced induced α-GalCer–induced hepatic injury (12); in fact, TNF-α is thought to play a critical role in α-GalCer–induced liver injury. Therefore, we next examined TNF-α production in WT and IDO-KO mice treated with α-GalCer. TNF-α mRNA expression in the livers of IDO-KO mice was increased compared with that in the livers of WT mice at 12 h after α-GalCer treatment (Fig. 3*A*). Moreover, we measured plasma TNF-α levels up to 2 d after administration of 2 μg of α-GalCer to WT and IDO-KO mice by ELISA (Fig. 3*B*). The TNF-α levels peaked at 5 h after α-GalCer application in both WT mice and IDO-KO mice. How-

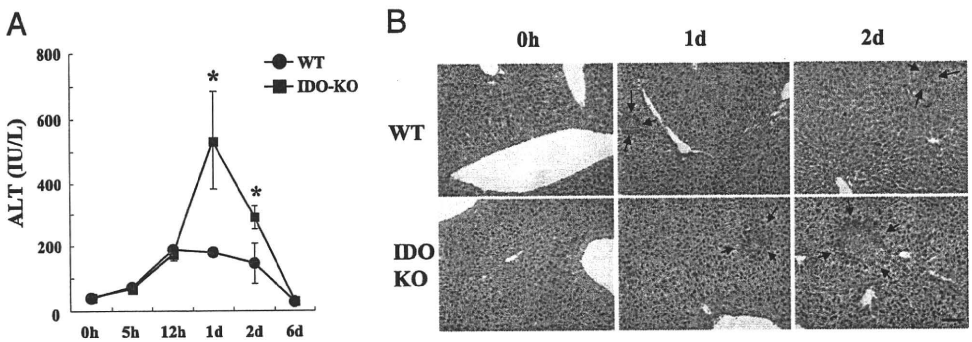

FIGURE 2. Induction of liver injury by α-GalCer in WT mice and IDO-KO mice. *A*, Serum ALT activity was measured at varying time points after α-GalCer injection into WT and IDO-KO mice. Each value is represented by the mean (SEM) of three mice. $*p < 0.05$. *B*, Histopathological characteristics of WT and IDO-KO mice livers observed at 0, 1, and 2 d after α-GalCer administration in these mice. H&E, original magnification ×200; scale bar, 100 μm. Arrows designate necroinflammatory foci in the liver. These experiments were repeated three times, and the same results were obtained.

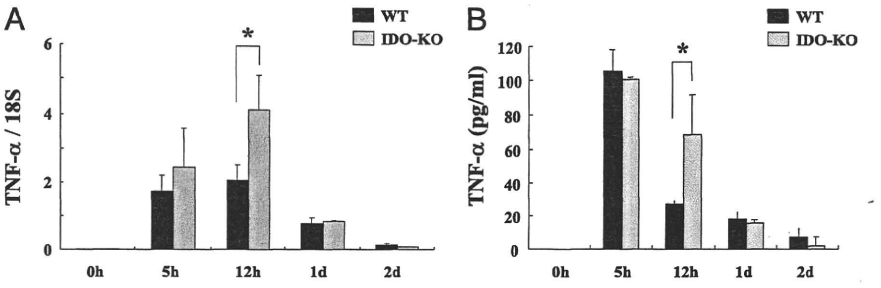

FIGURE 3. α-GalCer–induced TNF-α production in WT and IDO-KO mice. *A*, TNF-α mRNA expression in the livers of WT and IDO-KO mice that were administered α-GalCer. The mRNA level of TNF-α was normalized to that of 18S mRNA. Representative charts were derived from the analyses of three mice per group. *B*, Serum TNF-α concentration was determined by ELISA in WT and IDO-KO mice after α-GalCer injection. Each value is represented by the mean (SEM) of three mice. $*p < 0.05$.

ever, the concentration of TNF-α in IDO-KO mice was significantly increased compared with that in WT mice at 12 h after α-GalCer injection.

α-GalCer–induced cytokine and chemokine expression in WT mice and IDO-KO mice

As reported previously, NKT cells can produce a broad range of immunostimulatory or immunoregulatory cytokines and chemokines on activation, such as IL-2, IL-4, IL-10, IFN-γ, TNF-α, MIP-2, and KC (16–18). Therefore, we conducted a detailed time course analysis of the mRNA expression of intrahepatic cytokines (IFN-γ, IL-2, IL-4, IL-6, IL-10, and TGF-β) and chemokines (MIP-2, MCP-1, and KC) in WT and IDO-KO mice treated with α-GalCer (Fig. 4). Intrahepatic IL-6, MIP-2, and KC mRNA expression in IDO-KO mice was significantly increased compared with that in WT mice at 12 h after α-GalCer treatment. The marked differences between WT and IDO-KO mice were not observed with the mRNA expression of other cytokines and chemokines. Next, we measured the serum IL-6, MIP-2, and KC concentrations in WT and IDO-KO mice treated with α-GalCer. Although intrahepatic mRNA expressions of these

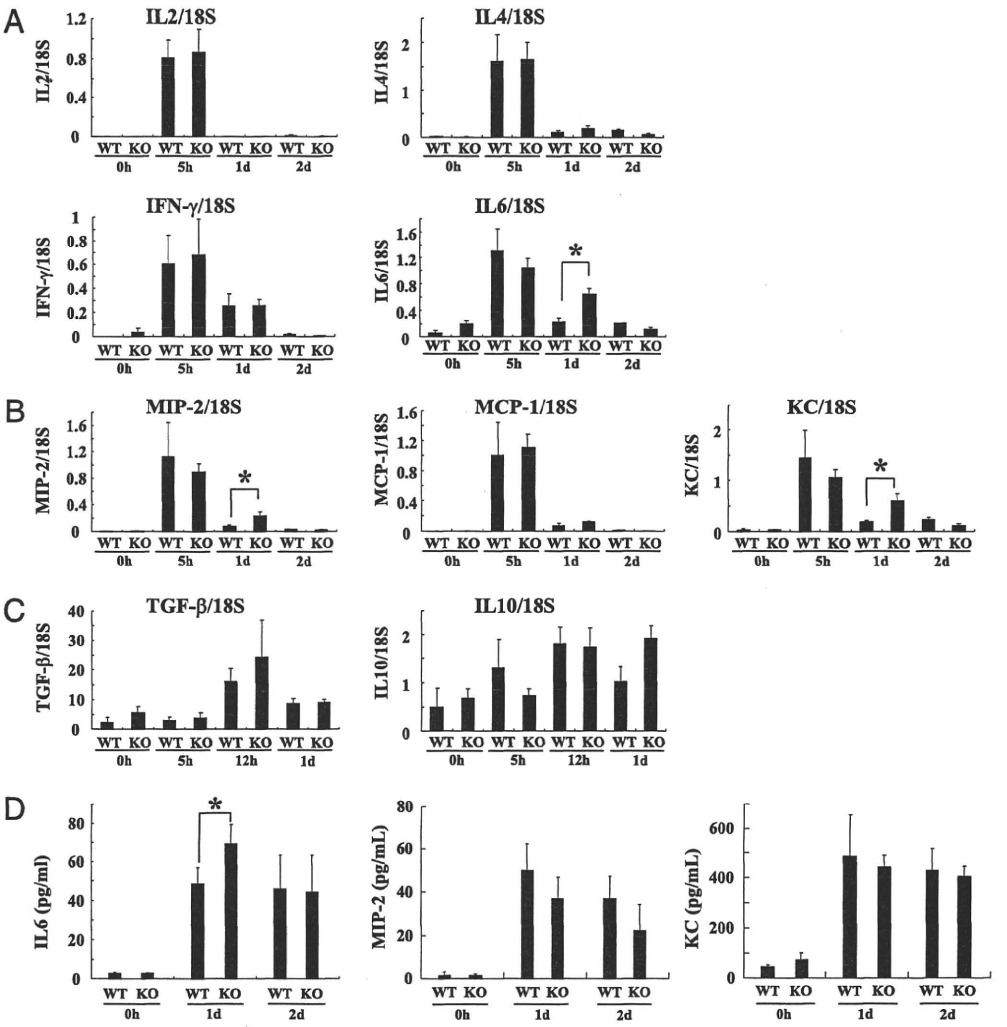

FIGURE 4. α-GalCer–induced cytokine and chemokine expression in WT mice and IDO-KO mice. *A*, IL-2, IL-4, IL-6, and IFN-γ mRNA expression in the livers of WT and IDO-KO mice that were administered α-GalCer. *B*, mRNA expression of chemokines (MIP-2, MCP-1, and KC) in the livers of WT and IDO-KO mice that were administered α-GalCer. *C*, TGF-β and IL-10 mRNA expression in the livers of WT and IDO-KO mice that were administered α-GalCer. The mRNA levels of cytokines and chemokines were normalized to those of 18S mRNA. *D*, Serum IL-6, MIP-2, and KC concentrations in WT and IDO-KO mice after α-GalCer injection were determined by ELISA. Representative charts derived from the analyses of three mice per group. $*p < 0.05$.

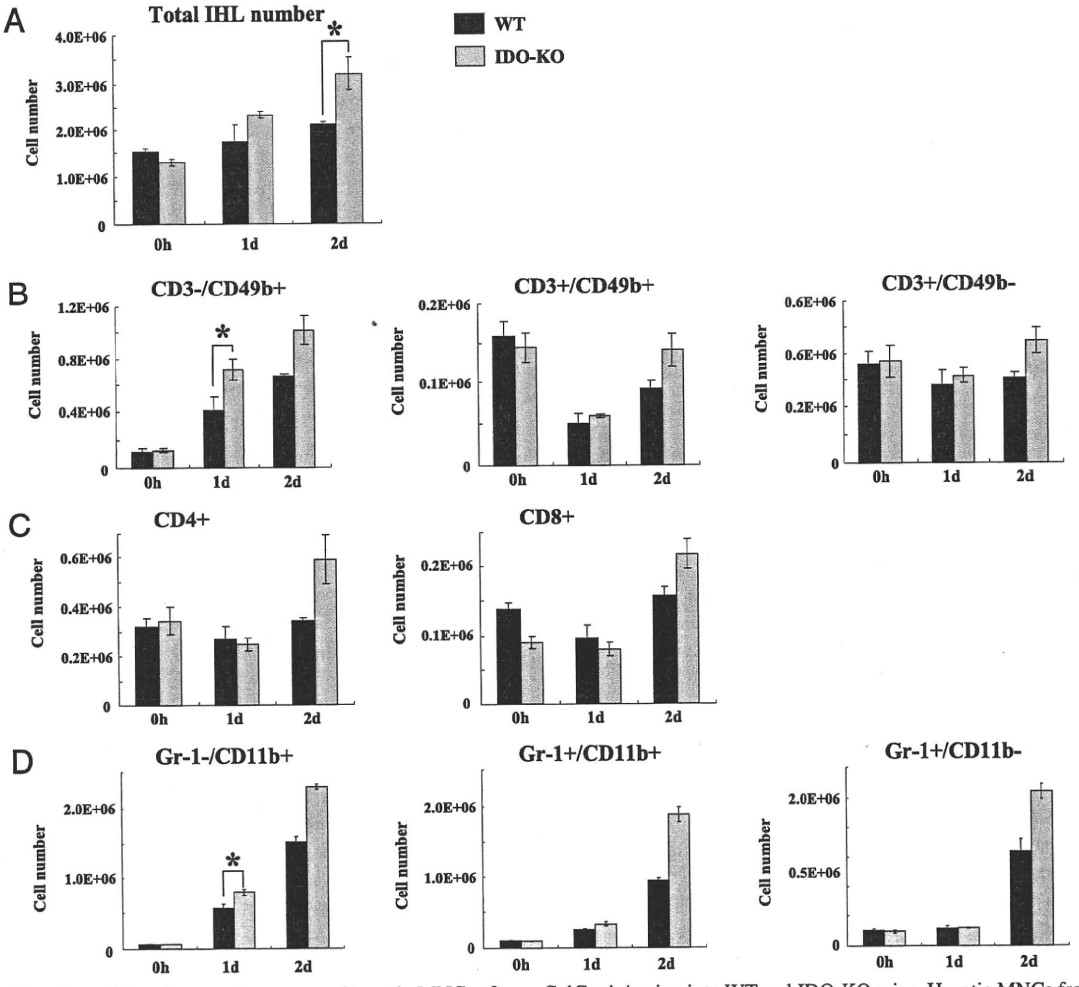

FIGURE 5. Kinetics and lymphocyte phenotypes of hepatic MNCs after α-GalCer injection into WT and IDO-KO mice. Hepatic MNCs from WT (black bars) and IDO-KO (gray bars) mice were obtained at 0, 1, and 2 d after α-GalCer injection. Cell numbers were quantified using FACScan analysis. *A*, Total number of hepatic MNCs after α-GalCer injection. *B*, Number of $CD3^-CD49b^+$ cells, $CD3^+CD49b^+$ cells, and $CD3^+CD49b^-$ cells after α-GalCer injection. *C*, Number of $CD4^+$ and $CD8^+$ cells after α-GalCer injection. *D*, Number of $CD11b^+Gr\text{-}1^-$ cells, $CD11b^+Gr\text{-}1^+$ cells, and $CD11b^-Gr\text{-}1^+$ cells at 1 d after α-GalCer injection. Results are presented as the mean number of cells of each cell type of hepatic MNCs for at least three mice per group. Error bars indicate the SEM. $*p < 0.05$. IHL, intrahepatic lymphocyte.

chemokines and cytokine in IDO-KO mice were increased compared with those in WT mice, the concentration of IL-6 in IDO-KO mice only elevated in serum.

Lymphocyte phenotypes of hepatic MNCs after α-GalCer injection into WT and IDO-KO mice

Next, we examined the lymphocyte phenotypes of hepatic MNCs from WT and IDO-KO mice treated with α-GalCer. The total number of MNCs in the livers of WT mice and IDO-KO mice was increased after α-GalCer injection. The increase in cell number was more enhanced in IDO-KO mice compared with WT mice at 2 d after α-GalCer injection (Fig. 5*A*). In particular, the frequency of hepatic $CD49b^+$ cells in IDO-KO mice significantly increased at 1 d after α-GalCer injection (Fig. 5*B*), coinciding with the peak of serum (Fig. 2). Although the number of $CD4^+$ and $CD8^+$ cells in the liver of IDO-KO mice increased compared with that in WT mice, the peak time was delayed compared with the peak time of liver injury in this model (Fig. 5*C*). Moreover, we measured the number of monocytes/macrophages in the liver from WT and IDO-KO mice after α-GalCer injection (Fig. 5*D*). The number of $CD11b^+Gr\text{-}1^-$ cells from IDO-KO mice was significantly increased compared with that from WT mice.

α-GalCer–induced TNF-α production in $CD49b^+$ and $CD11b^+$ cells

As shown in Fig. 5, we have confirmed that the number of $CD49b^+$ and $CD11b^+$ cells in the liver from IDO-KO mice treated with α-GalCer increased. Therefore, we measured the production of TNF-α on $CD49b^+$ and $CD11b^+$ cells by using intracellular cytokine staining (Fig. 6). $CD49b^+$ and $CD11b^+$ cells in the livers of both WT and IDO-KO mice significantly produced TNF-α at 12 h after α-GalCer injection. In particular, the number of TNF-α–producing cells in IDO-KO mice significantly increased compared with that in WT mice.

The IDO inhibitor 1-methyl-D-tryptophan enhances α-GalCer–induced liver injury

1-Methyl-D-tryptophan (1-MT) is a potent inhibitor of IDO, and hence we used this agent to substantiate data obtained with IDO-KO mice. WT mice were administered 1-MT orally at 0 or 5 mg/ml in drinking water for 3 d before α-GalCer stimulation. This experiment was performed twice independently. In both experiments, the serum ALT level in WT mice treated with 1-MT was significantly elevated compared with that in WT mice not treated with 1-MT at 1 d after α-GalCer stimulation (Fig. 7). Therefore,

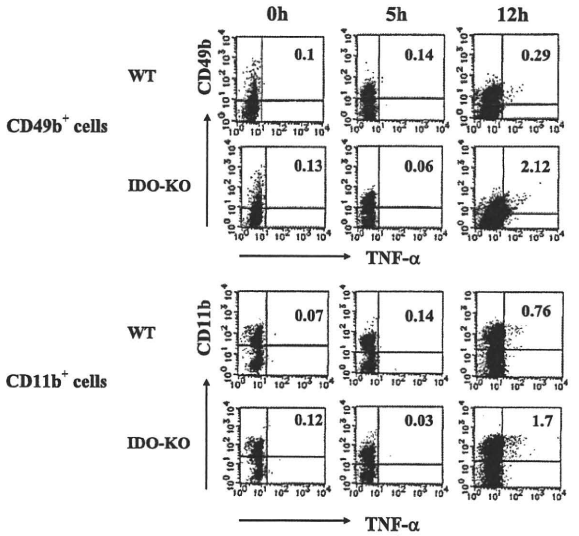

FIGURE 6. α-GalCer–induced TNF-α production in CD49b$^+$ and CD11b$^+$ cells. Flow cytometric analysis of intracellular TNF-α produced by hepatic CD49b$^+$ and CD11b$^+$ cells obtained from mice at 0, 5, and 12 h after α-GalCer injection and cultured for 4 h in brefeldin A. Data are representative of at least three independent experiments with similar results.

pharmacological inhibition of IDO with 1-MT is consistent with the exacerbated situation observed using IDO-KO mice.

Discussion

In this study, we report that α-GalCer–induced liver injury was exacerbated in IDO-KO mice, and that the exacerbation was accompanied by an increase in the number of intrahepatic TNF-α–producing MNCs. The serum ALT level was significantly augmented in IDO-KO mice compared with WT mice after α-GalCer injection. In parallel, TNF-α expression induced by α-GalCer injection was more enhanced in the livers of IDO-KO mice. Moreover, the number of intrahepatic CD49b$^+$ and CD11b$^+$ cells in IDO-KO mice treated with α-GalCer significantly increased compared with that in WT mice, and the cells from IDO-KO mice produced a large amount of TNF-α. These data indicated that deficiency of IDO increased the number of intrahepatic TNF-α–producing cells and exacerbated α-GalCer–induced liver injury. To the best of our knowledge, this is the first report describing the effects of IDO on acute hepatic injury.

IDO is an enzyme that is ubiquitously distributed in mammalian tissues and cells; that is, from L-Trp to *N*-formylkynurenine, which is further catabolized to L-Kyn. IDO production is induced by an IFN-γ–dependent and/or an IFN-γ–independent mechanism and other proinflammatory cytokines in the course of an inflammatory response in different cells, including macrophages, fibroblasts, and epithelial cells (3, 4). Previous studies on IDO have demonstrated that the role that IDO plays in regulating immune responses has been the subject of intense investigation. The bulk of the literature has focused on investigating the suppressive effects of IDO activity, predominantly on the activation of T cells (1). The prevailing theory is that IDO expressed by dendritic cells inhibits T cell activation, either directly or indirectly, by driving the development of regulatory T cells.

Inhibition of IDO activity during immune-mediated colitis has recently been reported to markedly worsen disease in the gut (19). In sharp contrast, IDO can act as a mediator of inflammatory disease, particularly in ischemia-reperfusion injury (20). Additionally, it was reported that administration of 1-MT to K/BxN mice reduced the level of inflammatory cytokines and autoantibodies, resulting in an attenuated course of arthritis (21). Thus, IDO has contrasting effects on several types of inflammation models. However, the effects of IDO function in the acute murine liver injury model remain unknown. In this study, we used the α-GalCer–induced liver injury model to examine the role of IDO an acute liver injury.

We first confirmed the expression of IDO in the liver after α-GalCer administration (Fig. 1). IDO is induced by IFN-γ and other proinflammatory cytokines, whereas such proinflammatory cytokines are secreted in mice treated with α-GalCer (15, 17). In particular, immunohistochemical examination revealed that IDO expression was enhanced in hepatocytes after α-GalCer treatment (Fig. 1*D*). These results coincide with our previous data in which murine recombinant IFN-γ induced IDO mRNA expression in primary hepatocytes in vitro (8).

In this study, using IDO-KO mice, we clearly demonstrated that the IDO deficiency caused the exacerbation of liver injury in this murine α-GalCer–induced hepatitis model (Fig. 2). As shown in Fig. 1*D*, the expression of IDO in the liver was enhanced 1 d after α-GalCer treatment, and ALT level also increased simultaneously. These results indicate that IDO expression may partially regulate the liver injury. Moreover, 1-MT, a competitive inhibitor of IDO, also exacerbated liver injury in this hepatitis model (Fig. 7). Induction of IDO by α-GalCer treatment may thus suppress the increased immune response observed in acute liver injury and attenuate the liver injury caused in this model.

Previous studies have reported that TNF-α is an important mediator in the α-GalCer–induced liver injury model (12, 22, 23). Intrahepatic NKT cells and NK cells mainly secrete TNF-α after α-GalCer injection. Although intrahepatic macrophages/monocytes are known as a pivotal source of TNF-α, they are not essential for α-GalCer–mediated hepatotoxicity (12). In this study, TNF-α production in IDO-KO mice treated with α-GalCer was increased compared with that in WT mice, and TNF-α also played a critical role in this acute liver injury model (Fig. 3). In particular, TNF-α production in CD49b$^+$ and CD11b$^+$ cells from IDO-KO mice was

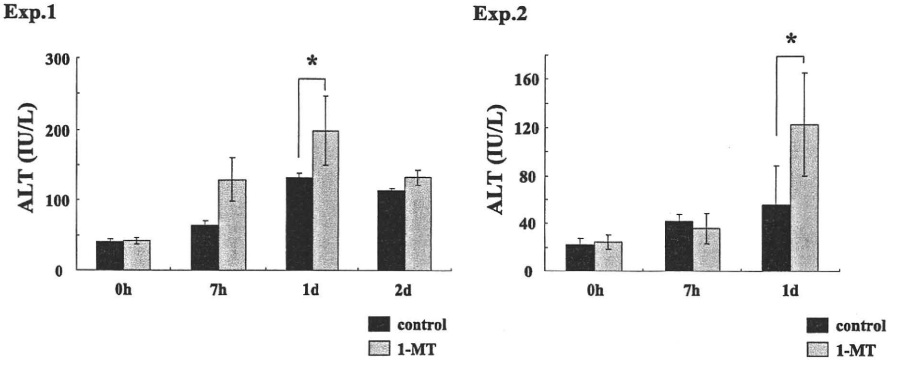

FIGURE 7. IDO inhibitor (1-MT) enhances α-GalCer–induced liver injury. IDO-WT mice were orally administered 1-MT at 0 or 5 mg/ml in drinking water for 3 d before α-GalCer stimulation. Serum ALT activity was analyzed at varying time points relative to the injection of α-GalCer into 1-MT–treated and nontreated mice. Representative charts were derived from the analyses of four or five mice per group. These experiments were independently performed twice (Exp. 1 and Exp. 2). Error bars indicate the SEM. $*p < 0.05$.

significantly increased compared with that from WT mice (Fig. 6). α-GalCer can enhance TNF-α production and cytotoxicity in NK cells and NKT cells (12, 24). The increase in the number of TNF-α–producing CD49b$^+$ cells (including NK cells and NKT cells) presumably contributes to the exacerbation of α-GalCer–induced liver injury. On the other hand, although the previous study demonstrated that macrophages/monocytes did not contribute to the progression of α-GalCer–mediated liver injury (12), TNF-α production in intrahepatic macrophages/monocytes from IDO-KO mice treated with α-GalCer was enhanced in our study. Therefore, we speculated that IDO may suppress TNF-α production in activated macrophages/monocytes.

It was previously reported that IDO induces inhibition of immune cell (e.g., NK cells and T cells) proliferation (25, 26). In our data, intrahepatic MNCs from IDO-KO mice treated with α-GalCer were apoptosis resistant with those from WT mice. Furthermore, the number of apoptotic splenocytes increased in the presence of WT hepatocytes on α-GalCer stimulation (Fig. 7). In contrast, apoptotic splenocytes did not increase in the presence of α-GalCer when splenocytes from IDO-KO mice were cultured with hepatocytes from IDO-KO mice. We suggested that activated intrahepatic MNCs may be resistant to apoptosis in the absence of IDO, and the number of intrahepatic MNCs in IDO-KO mice treated with α-GalCer increased compared with that in WT mice.

Real-time PCR analysis revealed that mRNA expression of IL-6, MIP-2, and KC in the liver of IDO-KO mice was upregulated at 24 h after α-GalCer injection (Fig. 4). There was no difference between WT and IDO-KO mice with regard to the α-GalCer reactivity, because the expression of cytokines and chemokines after α-GalCer injection was equally enhanced in the livers of WT and IDO-KO mice in the early phase (at 5 h) after α-GalCer injection. The lack of IDO promoted enhancement of IL-6, MIP-2, and KC expression in the late phase (at 24 h) after α-GalCer injection. However, there is no difference between WT and IDO-KO mice in serum MIP-2 and KC levels. These results indicated that expression of MIP-2 and KC may be affected by the expression of IDO only in the liver. Moreover, increased production of such cytokine and chemokines augments the number of intrahepatic NK cells and CD11b$^+$ cells, and they subsequently exacerbate liver injury in IDO-KO mice treated with α-GalCer. Taken together, we demonstrated that IDO inhibited not only the proliferation of NK cells and macrophages but also TNF-α production in these cells in the liver after administration of α-GalCer. IDO has the ability to suppress overactive immune response in the α-GalCer–induced hepatitis model.

In summary, this study demonstrated that IDO deficiency exacerbated liver injury in α-GalCer–induced hepatitis. IDO induced by proinflammatory cytokines may decrease the number of intrahepatic TNF-α–producing immune cells (NK cells and macrophages in particular) in acute hepatitis. Enhancement of IDO expression may suppress overactive immune response in the α-GalCer–induced hepatitis model. Accordingly, IDO regulation may be a therapeutic target in acute hepatitis.

Disclosures

The authors have no financial conflicts of interest.

References

1. Munn, D. H., E. Shafizadeh, J. T. Attwood, I. Bondarev, A. Pashine, and A. L. Mellor. 1999. Inhibition of T cell proliferation by macrophage tryptophan catabolism. *J. Exp. Med.* 189: 1363–1372.
2. Mellor, A. L., and D. H. Munn. 1999. Tryptophan catabolism and T-cell tolerance: immunosuppression by starvation? *Immunol. Today* 20: 469–473.
3. Taylor, M. W., and G. S. Feng. 1991. Relationship between interferon-γ, indoleamine 2,3-dioxygenase, and tryptophan catabolism. *FASEB J.* 5: 2516–2522.
4. Fujigaki, S., K. Saito, K. Sekikawa, S. Tone, O. Takikawa, H. Fujii, H. Wada, A. Noma, and M. Seishima. 2001. Lipopolysaccharide induction of indoleamine 2,3-dioxygenase is mediated dominantly by an IFN-γ-independent mechanism. *Eur. J. Immunol.* 31: 2313–2318.
5. Fallarino, F., U. Grohmann, K. W. Hwang, C. Orabona, C. Vacca, R. Bianchi, M. L. Belladonna, M. C. Fioretti, M. L. Alegre, and P. Puccetti. 2003. Modulation of tryptophan catabolism by regulatory T cells. *Nat. Immunol.* 4: 1206–1212.
6. Grohmann, U., F. Fallarino, R. Bianchi, C. Orabona, C. Vacca, M. C. Fioretti, and P. Puccetti. 2003. A defect in tryptophan catabolism impairs tolerance in nonobese diabetic mice. *J. Exp. Med.* 198: 153–160.
7. Terness, P., T. M. Bauer, L. Röse, C. Dufter, A. Watzlik, H. Simon, and G. Opelz. 2002. Inhibition of allogeneic T cell proliferation by indoleamine 2,3-dioxygenase-expressing dendritic cells: mediation of suppression by tryptophan metabolites. *J. Exp. Med.* 196: 447–457.
8. Iwamoto, N., H. Ito, K. Ando, T. Ishikawa, A. Hara, A. Taguchi, K. Saito, M. Takemura, M. Imawari, H. Moriwaki, and M. Seishima. 2009. Upregulation of indoleamine 2,3-dioxygenase in hepatocyte during acute hepatitis caused by hepatitis B virus-specific cytotoxic T lymphocytes in vivo. *Liver Int.* 29: 277–283.
9. Larrea, E., J. I. Riezu-Boj, L. Gil-Guerrero, N. Casares, R. Aldabe, P. Sarobe, M. P. Civeira, J. L. Heeney, C. Rollier, B. Verstrepen, et al. 2007. Upregulation of indoleamine 2,3-dioxygenase in hepatitis C virus infection. *J. Virol.* 81: 3662–3666.
10. Biburger, M., and G. Tiegs. 2008. Activation-induced NKT cell hyporesponsiveness protects from α-galactosylceramide hepatitis and is independent of active transregulatory factors. *J. Leukoc. Biol.* 84: 264–279.
11. Nakagawa, R., I. Nagafune, Y. Tazunoki, H. Ehara, H. Tomura, R. Iijima, K. Motoki, M. Kamishohara, and S. Seki. 2001. Mechanisms of the antimetastatic effect in the liver and of the hepatocyte injury induced by α-galactosylceramide in mice. *J. Immunol.* 166: 6578–6584.
12. Biburger, M., and G. Tiegs. 2005. α-Galactosylceramide-induced liver injury in mice is mediated by TNF-α but independent of Kupffer cells. *J. Immunol.* 175: 1540–1550.
13. Hoshi, M., H. Ito, H. Fujigaki, M. Takemura, T. Takahashi, E. Tomita, M. Ohyama, R. Tanaka, K. Saito, and M. Seishima. 2009. Indoleamine 2,3-dioxygenase is highly expressed in human adult T-cell leukemia/lymphoma and chemotherapy changes tryptophan catabolism in serum and reduced activity. *Leuk. Res.* 33: 39–45.
14. Ito, H., K. Ando, T. Ishikawa, K. Saito, M. Takemura, M. Imawari, H. Moriwaki, and M. Seishima. 2009. Role of TNF-α produced by nonantigen-specific cells in a fulminant hepatitis mouse model. *J. Immunol.* 182: 391–397.
15. Ito, H., K. Ando, T. Nakayama, M. Taniguchi, T. Ezaki, K. Saito, M. Takemura, K. Sekikawa, M. Imawari, M. Seishima, and H. Moriwaki. 2003. Role of Vα14 NKT cells in the development of impaired liver regeneration in vivo. *Hepatology* 38: 1116–1124.
16. Godfrey, D. I., K. J. Hammond, L. D. Poulton, M. J. Smyth, and A. G. Baxter. 2000. NKT cells: facts, functions and fallacies. *Immunol. Today* 21: 573–583.
17. Ito, H., K. Ando, T. Ishikawa, T. Nakayama, M. Taniguchi, K. Saito, M. Imawari, H. Moriwaki, T. Yokochi, S. Kakumu, and M. Seishima. 2008. Role of Vα14$^+$ NKT cells in the development of hepatitis B virus-specific CTL: activation of Vα14$^+$ NKT cells promotes the breakage of CTL tolerance. *Int. Immunol.* 20: 869–879.
18. Wintermeyer, P., C. W. Cheng, S. Gehring, B. L. Hoffman, M. Holub, L. Brossay, and S. H. Gregory. 2009. Invariant natural killer T cells suppress the neutrophil inflammatory response in a mouse model of cholestatic liver damage. *Gastroenterology* 136: 1048–1059.
19. Harrington, L., C. V. Srikanth, R. Antony, S. J. Rhee, A. L. Mellor, H. N. Shi, and B. J. Cherayil. 2008. Deficiency of indoleamine 2,3-dioxygenase enhances commensal-induced antibody responses and protects against *Citrobacter* rodentium-induced colitis. *Infect. Immun.* 76: 3045–3053.
20. Mohib, K., S. Wang, Q. Guan, A. L. Mellor, H. Sun, C. Du, and A. M. Jevnikar. 2008. Indoleamine 2,3-dioxygenase expression promotes renal ischemia-reperfusion injury. *Am. J. Physiol. Renal Physiol.* 295: F226–F234.
21. Scott, G. N., J. DuHadaway, E. Pigott, N. Ridge, G. C. Prendergast, A. J. Muller, and L. Mandik-Nayak. 2009. The immunoregulatory enzyme IDO paradoxically drives B cell-mediated autoimmunity. *J. Immunol.* 182: 7509–7517.
22. Minagawa, M., Q. Deng, Z. X. Liu, H. Tsukamoto, and G. Dennert. 2004. Activated natural killer T cells induce liver injury by Fas and tumor necrosis factor-α during alcohol consumption. *Gastroenterology* 126: 1387–1399.
23. Inui, T., H. Nakashima, Y. Habu, R. Nakagawa, M. Fukasawa, M. Kinoshita, N. Shinomiya, and S. Seki. 2005. Neutralization of tumor necrosis factor abrogates hepatic failure induced by α-galactosylceramide without attenuating its antitumor effect in aged mice. *J. Hepatol.* 43: 670–678.
24. Shimizu, K., A. Goto, M. Fukui, M. Taniguchi, and S. Fujii. 2007. Tumor cells loaded with α-galactosylceramide induce innate NKT and NK cell-dependent resistance to tumor implantation in mice. *J. Immunol.* 178: 2853–2861.
25. Frumento, G., R. Rotondo, M. Tonetti, G. Damonte, U. Benatti, and G. B. Ferrara. 2002. Tryptophan-derived catabolites are responsible for inhibition of T and natural killer cell proliferation induced by indoleamine 2,3-dioxygenase. *J. Exp. Med.* 196: 459–468.
26. Sarkhosh, K., E. E. Tredget, A. Karami, H. Uludag, T. Iwashina, R. T. Kilani, and A. Ghahary. 2003. Immune cell proliferation is suppressed by the interferon-γ-induced indoleamine 2,3-dioxygenase expression of fibroblasts populated in collagen gel (FPCG). *J. Cell. Biochem.* 90: 206–217.

Role of Acid Sphingomyelinase of Kupffer Cells in Cholestatic Liver Injury in Mice

Yosuke Osawa,[1,2] Ekihiro Seki,[3] Masayuki Adachi,[3] Atsushi Suetsugu,[2] Hiroyasu Ito,[1] Hisataka Moriwaki,[2] Mitsuru Seishima,[1] and Masahito Nagaki[2]

Kupffer cells, resident tissue macrophages of the liver, play a key role in the regulation of hepatic inflammation, hepatocyte death, and fibrosis that characterize liver diseases. However, it is controversial whether Kupffer cells promote or protect from liver injury. To explore this issue we examined the role of Kupffer cells in liver injury, cell death, regeneration, and fibrosis on cholestatic liver injury in C57BL/6 mice using a model of partial bile duct ligation (BDL), in which animals do not die and the effects of BDL can be compared between injured ligated lobes and nonligated lobes. In cholestatic liver injury, the remaining viable cells represented tolerance for tumor necrosis factor alpha (TNF-α)-induced hepatocyte apoptosis and regenerative features along with AKT activation. Inhibition of AKT by adenovirus expressing dominant-negative AKT abolished the survival and regenerative properties in hepatocytes. Moreover, Kupffer cell depletion by alendronate liposomes increased hepatocyte damage and the sensitivity of TNF-α-induced hepatocyte apoptosis in ligated lobes. Kupffer cell depletion decreased hepatocyte regeneration and liver fibrosis with reduced AKT activation. To investigate the impact of acid sphingomyelinase (ASMase) in Kupffer cells, we generated chimeric mice that contained ASMase-deficient Kupffer cells and -sufficient hepatocytes using a combination of Kupffer cell depletion, irradiation, and the transplantation of ASMase-deficient bone marrow cells. In these mice, AKT activation, the tolerance for TNF-α-induced apoptosis, and the regenerative responses were attenuated in hepatocytes after BDL. *Conclusion:* Kupffer cells have a protective role for hepatocyte damage and promote cell survival, liver regeneration, and fibrosis in cholestatic liver disease. Kupffer cell-derived ASMase is crucial for AKT activation of hepatocytes that is required for the survival and regenerative responses. (HEPATOLOGY 2010;51:237-245.)

Chronic liver disease is associated with inflammatory cell infiltration, cytokine production, and liver cell death. Persistent hepatocyte death impairs hepatocyte regeneration accompanied with excessive production of extracellular matrix proteins causing liver fibrosis. Kupffer cells, resident tissue macrophages of the liver, function as both a promoter and a protector against liver injury. Lipopolysaccharide activates Kupffer cells and induces liver injury and inhibition of Kupffer cells prevents liver injury.[1] In addition, inhibition of Kupffer cell activation prevents liver injury induced by melphalan[2] and fumonisin B1.[3] In contrast, reduced Kupffer cell activity augments some kinds of liver injuries, such as hepatectomy- or acetaminophen-induced liver injury.[4,5] Activated Kupffer cells release various types of inflammatory cytokines and growth factors,[6] and these mediators are thought to regulate liver injury and regeneration. Especially, tumor necrosis factor alpha (TNF-α) from activated Kupffer cells plays a major role in the pathogenesis of various liver injuries.[7,8] Cholestasis is associated with many liver diseases. Bile duct ligation (BDL) causes hepatocyte damage, hepatic stellate cell (HSC) activation, and liver fibrosis accompanied by Kupffer cell activation leading to the production of a variety of cytokines and chemokines that are involved in liver damage and fibrosis.[9-11] Because these features are similar to human cholestatic diseases,

Abbreviations: α-SMA, alpha smooth muscle actin; Ale-lip, liposome-encapsulated alendronate; ASMase, acid sphingomyelinase; BDL, bile duct ligation; DN, dominant negative; GalN, D-galactosamine; GSK, glycogen synthase kinase; HSC, hepatic stellate cell; PBDL, partial BDL; TNF-α, tumor necrosis factor alpha; TUNEL, terminal deoxynucleotidyl transferase nick end-labeling.

From the [1]Department of Informative Clinical Medicine, Gifu University Graduate School of Medicine, Gifu, Japan; [2]Department of Gastroenterology, Gifu University Graduate School of Medicine, Gifu, Japan; [3]Department of Medicine, University of California San Diego, School of Medicine, La Jolla, CA, USA.

Received April 23, 2009; accepted August 23, 2009.

Supported by Grant-in-Aid from the Ministry of Education, Culture, Sports, Science, and Technology of Japan (19790478) (21790657) (both to Y.O.) and by a Liver Scholar Award from the AASLD/ALF (to E.S.).

Address reprint requests to: Yosuke Osawa M.D. PhD., Department of Informative Clinical Medicine, Gifu University Graduate School of Medicine, 1-1 Yanagido Gifu, 501-1194, Japan. E-mail:osawa-gif@umin.ac.jp; fax: 81-58-230-6431.

Published online in Wiley InterScience (www.interscience.wiley.com).

DOI 10.1002/hep.23262

Potential conflict of interest: Nothing to report.

Additional Supporting Information may be found in the online version of this article.

common BDL has been used as an animal model of chronic liver disease. However, in this model, common bile duct ligation causes total bile acid reflux to damage whole liver, and the animals show high mortality due to liver failure. We have previously established a partial BDL (PBDL) model, in which animals showed a typical liver injury only in the BDL lobes but no damage in the nonligated lobes with viable liver functions. In this study we examined the role of Kupffer cells in chronic liver injury using the PBDL model.

Acid sphingomyelinase (ASMase) hydrolyses sphingomyelin into ceramide and phosphorylcholine and is involved in various cell functions. Ceramide has been identified as a bioactive mediator of various cellular functions.[12] In addition, roles for sphingomyelin and ceramide in membrane lipid rafts have been reported,[13] which is related with transmitting signals across the plasma membrane. In macrophages, ASMase contributes to cytokine and chemokine release. Its inhibitor, sphingomyeline difluoromethylene analogue-7 (SMA-7), suppressed lipopolysaccharide-induced releases of TNF-α, interleukin (IL)-1β, and IL-6 from macrophages, and it reduces the severity of inflammatory bowel disease induced by dextran sodium sulfate.[14] In contrast, production of macrophage inflammatory protein-1α and -2 is increased in ASMase-deficient macrophages.[15] In addition, ASMase-deficient macrophage is impaired in killing bacteria.[16] Thus, ASMase contributes to various immunoresponses. In liver damage, although deficiency of ASMase leads to resistance to hepatocyte cell death induced by TNF-α,[17,18] the role of ASMase in Kupffer cells remains unclear.

In this study we assessed the roles of Kupffer cells and ASMase during chronic liver injury using PBDL mice. We found that Kupffer cells reduce liver damage, and induce hepatocyte survival and regeneration, and fibrosis. The protective and regenerative effects require AKT in hepatocytes by way of ASMase in Kupffer cells.

Materials and Methods

Animals and PBDL. ASMase knockout mice (ASMase$^{-/-}$) (C57Bl/6 background)[18] were bred for studies. Eight-week-old male wildtype C57Bl/6J mice were obtained from Japan SLC (Japan). The left hepatic duct was ligated for PBDL as reported.[19] The animals were fasted for 12 hours before sacrifice at 10 days after the surgery. As necessary, hepatocyte apoptosis was induced by mouse TNF-α (R&D Systems, Minneapolis, MN) (0.5 μg/mouse intravenously) with D-galactosamine (GalN) (Nacalai Tesque, Japan) (20 mg/mouse intraperitoneally) 10 days after the PBDL[20] and the animals were killed 6 hours after TNF-α administration. All procedures were approved by the Institutional Animal Care Committee of Gifu University.

Depletion of Kupffer Cells. Alendronate was reported to deplete Kupffer cells.[1] A single injection of liposome-encapsulated alendronate (Ale-lip) depleted F4/80-positive cells in the liver at 2-3 days after injection and the cells started to restore at 6 days (Supporting Fig. 1A). Ale-lip had no effect on hepatocytes with hematoxylin and eosin (H&E) (Supporting Fig. 1B) and alanine transaminase (ALT) (data not shown). The vitamin A autofluorescence and desmin-positive cells, characteristic features of HSCs, were not decreased by Ale-lip (Supporting Fig. 1CD). Ale-lip was injected to the operated mice 3 times at 1 day before surgery and 3 and 6 days after the surgery. Phosphate-buffered saline (PBS) encapsulated liposomes (PBS-lip) were used for control.

Bone Marrow Transplantation. Bone marrow transplantation was performed as reported.[11] The wildtype mice received Ale-lip injection twice at 1 and 4 days prior to lethal irradiation (11 Gy). Total bone marrow cells were collected from wildtype or ASMase$^{-/-}$ mice and injected to the irradiated recipient mice (10^7 cells). PBDL was performed 10 weeks after the transplantation.

Other Experimental Procedures. Other experimental procedures are described in the Supporting experimental procedures. These include preparation of liposome-encapsulated alendronate, adenovirus infection, histological analysis, western blot, quantitative real-time reverse-transcription polymerase chain reaction (RT-PCR), hydroxyproline measurement, and statistical analysis.

Results

Kupffer Cell Depletion Increases Hepatocellular Damage Induced by BDL. To examine the effect of Kupffer cell depletion on chronic liver damage induced by BDL, we initially injected Ale-lip three times to mice operated on with common BDL. Although the treatment with Ale-lip alone did not induce liver injury, the mortality of mice treated with common BDL and Ale-lip was extremely high; 40% 10 days after the surgery. In our established model, PBDL showed liver injury and fibrosis only in BDL lobes, which improved the survival rate up to 100% in Ale-lip-treated mice. Therefore, we decided to use PBDL for this study. In BDL lobes, F4/80-positive cells were increased. The Ale-lip treatment succeeded in deleting F4/80-positive cells (Fig. 1A). Thus, Ale-lip injection can be utilized as a new tool for Kupffer cell depletion. Inflammatory cytokines mainly produced from Kupffer cells were up-regulated in BDL lobes, whereas the

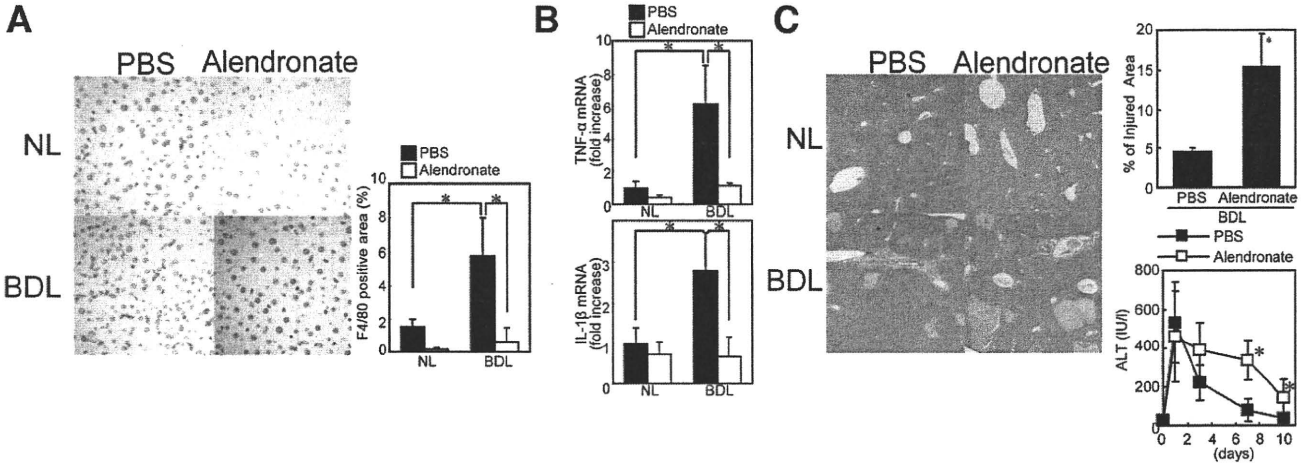

Fig. 1. Depletion of Kupffer cells increased liver injury after BDL. Wildtype mice were subjected to PBDL and treated with Ale-lip or PBS-lip. The animals were killed 10 days after the surgery. (A) Expression of F4/80 in the nonligated (NL) right (upper panel) and BDL left (lower panel) lobes was examined by immunohistochemistry. (Original magnification ×400; graph, right panel.) (B) Hepatic mRNA levels of TNF-α and IL-1β were determined by quantitative real-time RT-PCR. (C) The injured lesion in the ligated left lobes was assessed by H&E staining. (Original magnification ×40; graph, right upper panel.) Serum ALT levels were compared on the indicated time periods. Data are means ± SD from at least four independent experiments. *$P < 0.05$ using Student's t test.

Ale-lip treatment markedly inhibited the production of TNF-α and IL-1β (Fig. 1B). Kupffer cell-depleted mice showed an increase of injured lesion in BDL lobes and serum ALT level after the surgery (Fig. 1C). Interestingly, 24 hours after common BDL (Supporting Fig. 2) as well as PBDL (Fig. 1C), there were no significant differences in histological liver injury and elevated ALT activities between control and Kupffer cell-depleted mice. These findings indicate that Kupffer cells were not involved in the early stage of liver damage that occurs by BDL, but in the late stage.

Kupffer Cells Mediate Survival and Regeneration of Hepatocyte by BDL. As previously reported,[20] treatment with TNF-α plus GalN strongly induced hepatocyte destruction and massive hemorrhage with apoptotic cells in nonligated lobes of PBDL animals, whereas hemorrhagic damage and hepatocyte apoptosis were blunted in BDL lobes (Supporting Fig. 3A-C). Kupffer cell depletion itself did not induce hepatocyte apoptosis (Supporting Fig. 3D). In Kupffer cell-depleted livers, GalN plus TNF-α treatment induced hemorrhagic liver damage and hepatocyte apoptosis with the cleavage of poly (ADP-ribose) polymerase (PARP), which is the downstream target of caspase-3, both in nonligated and BDL lobes (Fig. 2A-C).

In the BDL lobes, proliferation cell nuclear antigen (PCNA) or Ki67-positive hepatocytes were increased with up-regulation of cyclin E expression (Fig. 2D-F), indicating that BDL induces hepatocyte regeneration. In Kupffer cell-depleted livers the expressions of PCNA, Ki67, and cyclin E were decreased (Fig. 2D-F). Thus, Kupffer cells are important for survival and regeneration of hepatocytes after BDL.

Kupffer Cells Are Required for Liver Fibrosis. Fibrosis was induced in BDL lobes as demonstrated by Sirius red staining, hydroxyproline content, expression of α-smooth muscle actin (α-SMA) and desmin, and messenger RNA (mRNA) expression of collagen-α1(I) and transforming growth factor (TGF)-β1 (Fig. 3). Kupffer cell-depleted mice showed reduced fibrosis in BDL lobes (Fig. 3). The number and the activation of HSCs were decreased by Kupffer cell depletion as assessed by desmin and α-SMA expression, respectively. These results suggest that the decrease in the fibrogenic response by Kupffer cell depletion is due to a lack of signal from Kupffer cells to activate and proliferate HSCs.

ASMase Deficiency in Kupffer Cells Diminishes the BDL-Induced Survival and Proliferative Effect. To further elucidate the mechanisms by which Kupffer cells contribute to BDL-mediated functional changes in liver injury, survival of hepatocyte, regeneration, and fibrosis, we focused on ASMase. The protein level of ASMase (Supporting Fig. 4) and ceramides (Supporting Table 1), the metabolite of ASMase, were increased in BDL lobes compared with those in nonligated lobes, suggesting the contribution of ASMase in the liver. To explore the involvement of ASMase in bone marrow-derived cells we generated ASMase-chimeric mice using a combination of alendronate-induced Kupffer cell depletion, irradiation, and bone marrow transplantation. To confirm the substitution of Kupffer cells in chimeric mice we initially generated the mice transplanted with bone marrow isolated

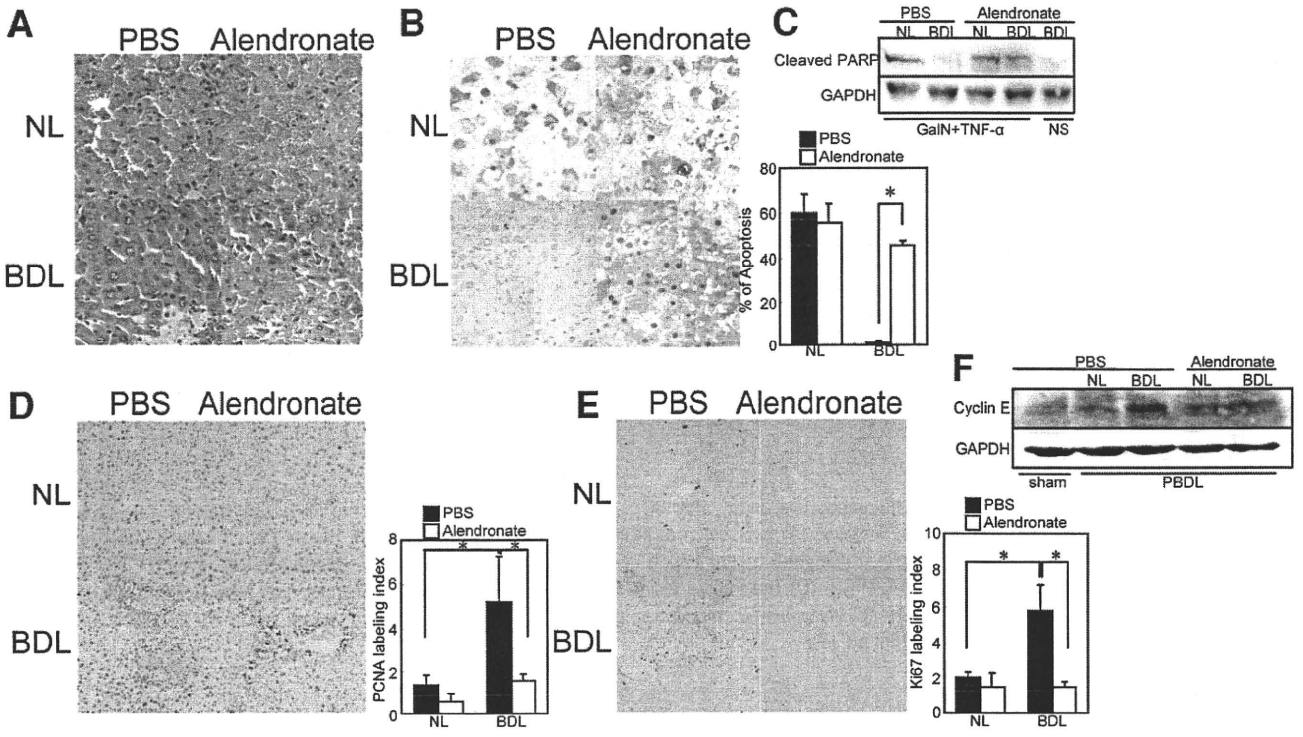

Fig. 2. Depletion of Kupffer cells abolished the survival effect of BDL and decreased hepatocyte regeneration after BDL. Wildtype mice were subjected to PBDL and treated with Ale-lip or PBS-lip. The animals were administered with (A-C) or without (D-F) GalN plus TNF-α (6 hours) on 10 days after the surgery. (A) Liver sections from the nonligated (NL) right (upper panel) and BDL left (lower panel) lobes were stained with H&E. (B) Apoptotic nuclei were identified using TUNEL staining. (Original magnification $\times$400; graph, right panel.) Expression of PCNA (D) and Ki67 (E) in the NL right (upper panel) and the BDL left (lower panel) lobes were examined by immunohistochemistry. (Original magnification $\times$200.) PCNA and Ki67 indexes were compared (right panel). Data are means $\pm$ SD from at least four independent experiments. *$P < 0.05$ using Student's t test. (C,F) The protein extracts from the NL and BDL lobes were subjected to sodium dodecyl sulfate-polyacrylamide gel electrophoresis (SDS-PAGE) and immunoblotting was performed with anti-PARP, cyclin E, and GAPDH antibodies. The results shown are representative of at least three independent experiments. NS, normal saline.

from β-actin promoter-driven green fluorescent protein (GFP)-transgenic mice. In the GFP-chimeric mouse liver all F4/80-positive cells were GFP-positive (Supporting Fig. 5A), suggesting that this protocol achieved full reconstitution of Kupffer cells to bone marrow-derived cells. The chimeric mice containing ASMase$^{-/-}$ bone marrow cells showed an increase of F4/80-positive cells, and TNF-α and IL-1β production after BDL, which were comparable to ASMase$^{+/+}$ bone marrow-transplanted mice (Supporting Fig. 5BC).

ASMase$^{-/-}$ bone marrow-transplanted mice showed an increase of liver injury in BDL lobes at the same degree as ASMase$^{+/+}$ bone marrow-transplanted mice (Fig. 4), suggesting that ASMase of Kupffer cell is not implicated in the liver injury. Hemorrhagic liver damage and apoptosis with PARP cleavage by GalN plus TNF-α were observed in BDL lobes of ASMase$^{-/-}$ bone marrow-transplanted mice but not in that of ASMase$^{+/+}$ bone marrow-transplanted mice (Fig. 5A-C). An increase of PCNA or Ki67-positive cells with cyclin E expression were blunted in BDL lobes of ASMase$^{-/-}$ bone marrow-transplanted mice (Fig. 5D-F). These results suggest that ASMase in Kupffer cells contribute to the protection against apoptosis and regeneration in BDL lobes. However, there was no difference between ASMase$^{-/-}$ bone marrow and ASMase$^{+/+}$ bone marrow-transplanted mice in mRNA expression of fibrogenic markers, Sirius red staining, and hydroxyproline content (Fig. 6). Thus, ASMase of Kupffer cell was not associated with liver fibrosis.

AKT Activation of Hepatocytes Is Required for Survival and Regeneration in BDL Lobes. Our previous study demonstrated that AKT was up-regulated in BDL lobes and was involved in hepatocyte survival from TNF-α-induced cell death.[20] In BDL lobes, phosphorylated-AKT and its downstream target, phosphorylated-glycogen synthase kinase (GSK)3β were increased (Supporting Fig. 6A). Immunohistochemical analysis identified that AKT in hepatocytes was phosphorylated (Supporting Fig. 6B). The AKT activation in BDL lobes was abrogated by the infection of Ad5 dominant negative (DN)-AKT (Supporting Fig. 6C). The inhibition of AKT abolished the survival effect (Supporting Fig. 6D) as re-

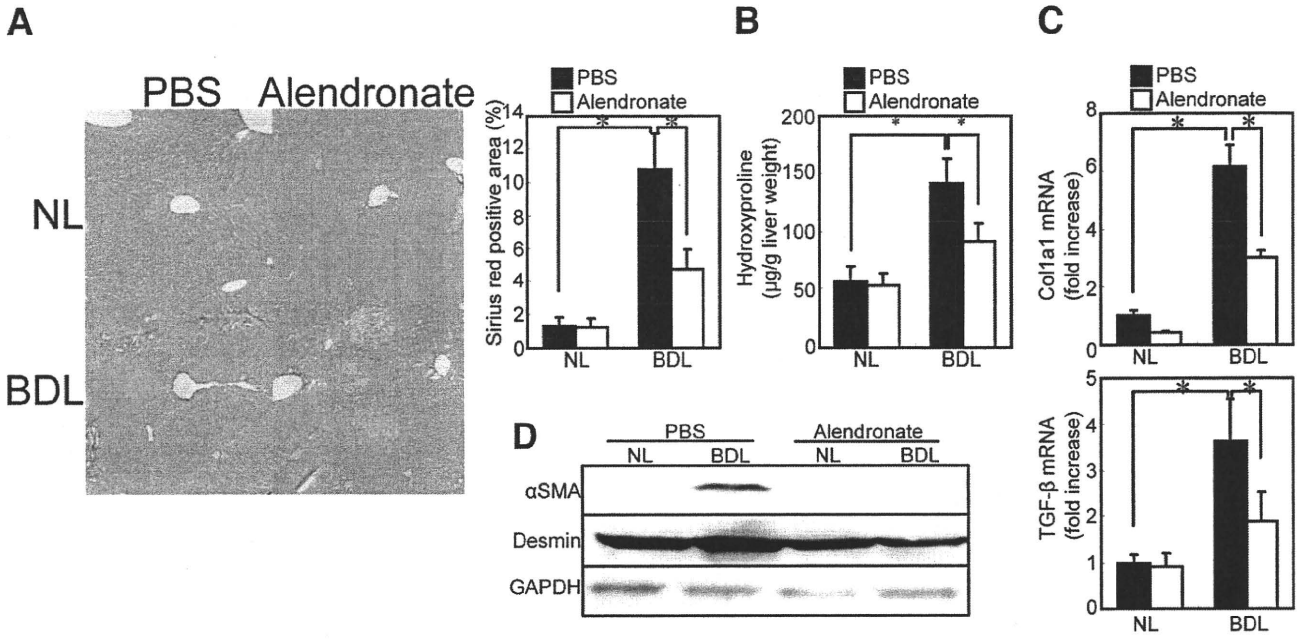

Fig. 3. Depletion of Kupffer cells reduced liver fibrosis after BDL. Wildtype mice were operated on with PBDL and treated with Ale-lip or PBS-lip. The animals were killed 10 days after the surgery. (A,B) Collagen deposition was assessed by Sirius red staining (original magnification ×100; graph, right panel) and measurement of hydroxyproline content. (C) mRNA levels of collagen α1(I) (col1α1) and TGF-β1 (TGF-β) in the livers were determined by quantitative real-time RT-PCR. Data are means ± SD from at least four independent experiments. $*P < 0.05$ using Student's t test. (D) The protein extracts from the livers were subjected to SDS-PAGE and immunoblotting was performed with anti-α-SMA, desmin, and GAPDH antibodies. The results shown are representative of at least three independent experiments.

ported,[20] and eliminated the induction of Ki67-positive cells and cyclin E (Fig. 7A,B) induced by BDL. These findings suggest that AKT activation in hepatocytes is essential for hepatocyte survival and regeneration observed in BDL lobes. In Kupffer cell-depleted mice (Fig. 7C) or ASMase$^{-/-}$ bone marrow-transplanted mice (Fig. 7D), the phosphorylation of AKT and GSK3β by BDL was inhibited. Thus, Kupffer cells and their ASMase are required for AKT-mediated survival and regeneration induced by BDL. Mcl-1 induction, which is a Bcl-2 family member and was regulated by AKT in hepatocytes (Supporting Fig. 6C,E),[21] was diminished in Kupffer cell-depleted mice or ASMase$^{-/-}$ bone marrow-transplanted mice, whereas Bcl-XL or Bfl-1 were not affected. These results suggest that survival may be mediated by Mcl-1 at the downstream of AKT.

Discussion

The present study specifically addressed the role of Kupffer cells and of ASMase in the cholestatic liver injury. Our results demonstrate that depletion of Kupffer cells

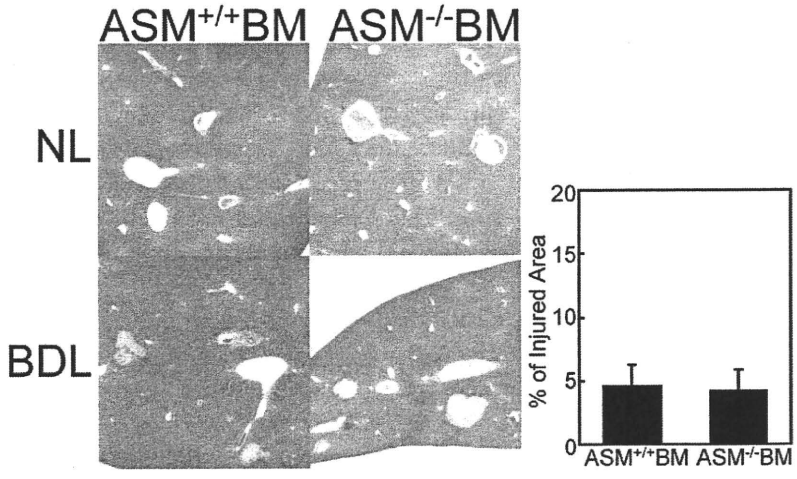

Fig. 4. Reconstitution of Kupffer cells with ASMase knockout cells did not affect on the liver injury induced by BDL. The ASMase$^{+/+}$ bone marrow or ASMase$^{-/-}$ bone marrow-transplanted mice were subjected to PBDL and killed 10 days after the surgery. Measurement of injured lesion in the BDL lobes was assessed with H&E. (Original magnification ×40; graph, right panel.) Data are means ± SD from at least four independent experiments.

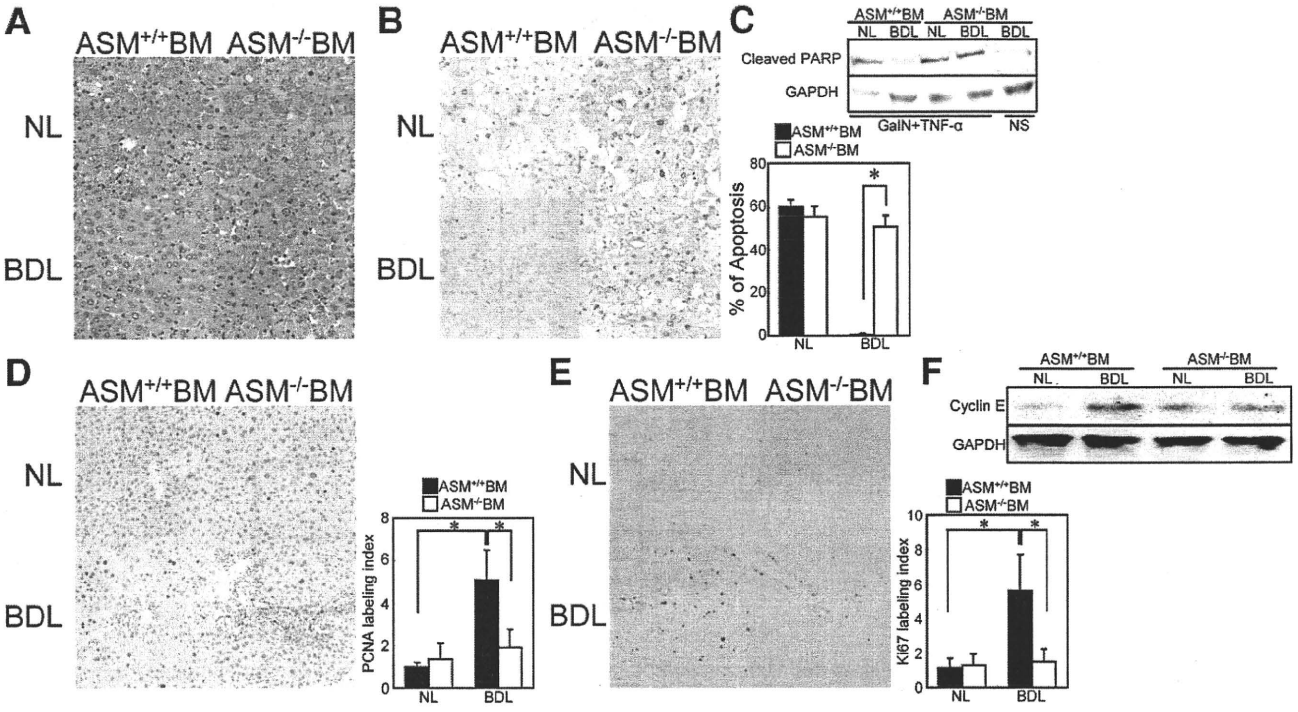

Fig. 5. Reconstitution of Kupffer cells to ASMase knockout cells abrogated the survival effect of BDL and decreased hepatocyte regeneration after BDL. The ASMase$^{+/+}$ bone marrow or ASMase$^{-/-}$ bone marrow-transplanted mice were operated on with PBDL and treated with (A-C) or without (D-F) GalN plus TNF-α treatment (6 hours) 10 days after the surgery. (A) Liver sections were stained with H&E. (B) Apoptotic nuclei were identified using TUNEL staining. (Original magnification $\times$400; graph, right panel.) Expression of PCNA (D) and Ki67 (E) in the nonligated (NL) right (upper panel) and the BDL left (lower panel) lobes was examined by immunohistochemistry. (Original magnification $\times$200.) PCNA and Ki67 indexes were compared (right panel). Data are means $\pm$ SD from at least four independent experiments. *$P < 0.05$ using Student's t test. (C,F) The protein extracts from the NL and BDL lobes were subjected to SDS-PAGE and immunoblotting was performed with anti-PARP, anti-cyclin E, and GAPDH antibodies. The results shown are representative of at least four independent experiments. NS, normal saline.

increased liver injury and susceptibility to TNF-α-induced hepatocyte apoptosis, and decreased hepatocyte regeneration and liver fibrosis with reduced AKT activation. Kupffer cell-derived ASMase was crucial for the AKT activation. The results raise novel therapeutic possibilities for treating liver injury.

After BDL, hepatocytes are exposed to elevated concentrations of bile acid, and hydrophobic bile acids lead to hepatocyte cell death[22] through various factors such as reactive oxygen species (ROS) generation from mitochondria[23] and activation of Fas signaling in a ligand-independent manner by altering cellular trafficking of Fas.[24] Indeed, expression of 4-hydroxy-2-nonenal (HNE), which is produced by lipid peroxidation, was increased on 1 day after the surgery of BDL (data not shown). Because Kupffer cell depletion did not increase the initial liver damage by BDL (1 day after the surgery), it is likely that this damage is induced by a direct toxic effect of bile acid rather than subsequent immune responses because Kupffer cells are not activated in this early stage. The initial hepatocyte cell death stimulates subsequent inflammatory responses leading to further liver injury and fibrosis.[25,26] In BDL liver, the engulfment of apoptotic or necrotic body in Kupffer cells is observed,[27] which leads to production of cytokines including TNF-α and TGF-β.[9] Either a promotive[9] or protective[10] effect of Kupffer cells on BDL-induced liver injury have been reported. In the present study, alendronate treatment, which depleted Kupffer cells in the livers, increased liver injury and reduced fibrosis 10 days after BDL, suggesting that Kupffer cells have a protective effect on the subsequent damage of hepatocytes and a promotive effect on fibrosis in the late stage. The increase of liver injury is probably explained by the diminished Kupffer cell functions, including the phagocytosis of injured tissue and the production of protective factors for hepatocytes. The reduced fibrosis is most likely due to decreased fibrogenic cytokines from Kupffer cells. Cytokines including TGF-β and TGF-α are released from Kupffer cells,[28] and HSCs are stimulated to induce collagen I α1 transcription by TGF-β.[29]

In the liver chronically injured by BDL, hepatocytes represented the survival and regenerative properties, and AKT was a critical factor for the survival and regeneration of the remaining viable hepatocytes. Indeed, overexpression of constitutive active-AKT led hepatocytes to be re-

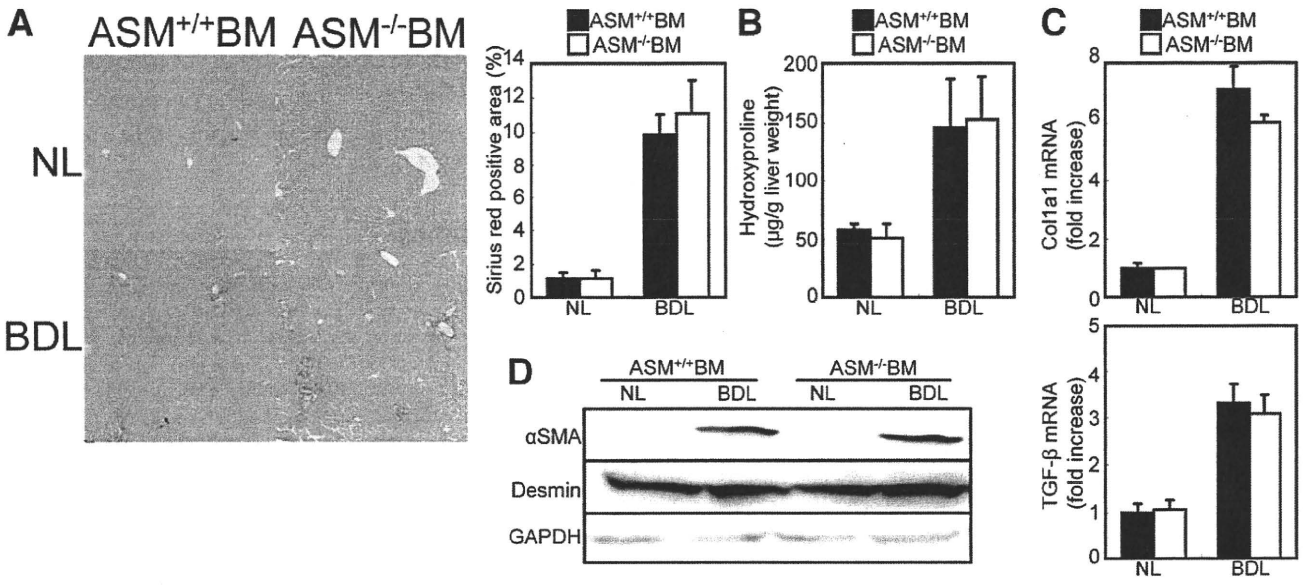

Fig. 6. Reconstitution of Kupffer cells to ASMase knockout cells did not affect the liver fibrosis induced by BDL. The ASMase$^{+/+}$ bone marrow or ASMase$^{-/-}$ bone marrow-transplanted mice were operated on with PBDL and killed 10 days after the surgery. (A,B) Collagen deposition was assessed by Sirius red staining (A) (original magnification ×100; graph, right panel) and measurement of hydroxyproline content (B). (C) mRNA levels of collagen α1(I) (col1a1) and TGF-β1 (TGF-β) in the livers were determined by quantitative real-time RT-PCR. Data are means ± SD from at least five independent experiments. (D) The protein extracts from the livers were subjected to SDS-PAGE and immunoblotting was performed with anti-α-SMA, desmin, and GAPDH antibodies. The results shown are representative of at least three independent experiments.

sistant against TNF-α-induced apoptosis in primary cultured hepatocytes (data not shown) and promoted hepatocyte proliferation by cyclin E.[30] Because depletion of Kupffer cells diminished the survival and regeneration of hepatocytes with reduced AKT activation, Kupffer cells could produce factors that activate AKT in hepatocytes. In our study, the survival and regenerative effects of AKT activation were abrogated in ASMase$^{-/-}$ bone marrow-transplanted mice, suggesting that ASMase in Kupffer cells requires the production of unknown factors that lead to the activation of AKT in hepatocytes. mRNA expression of TNF-α, IL-1β, and IL-6 in ASMase$^{-/-}$ bone marrow-transplanted mice were similar to those in ASMase$^{+/+}$ bone marrow-transplanted mice (Supporting Fig. 5 and data not shown) after BDL. mRNA levels of hepatocyte growth factor (HGF) and heparin-binding ep-

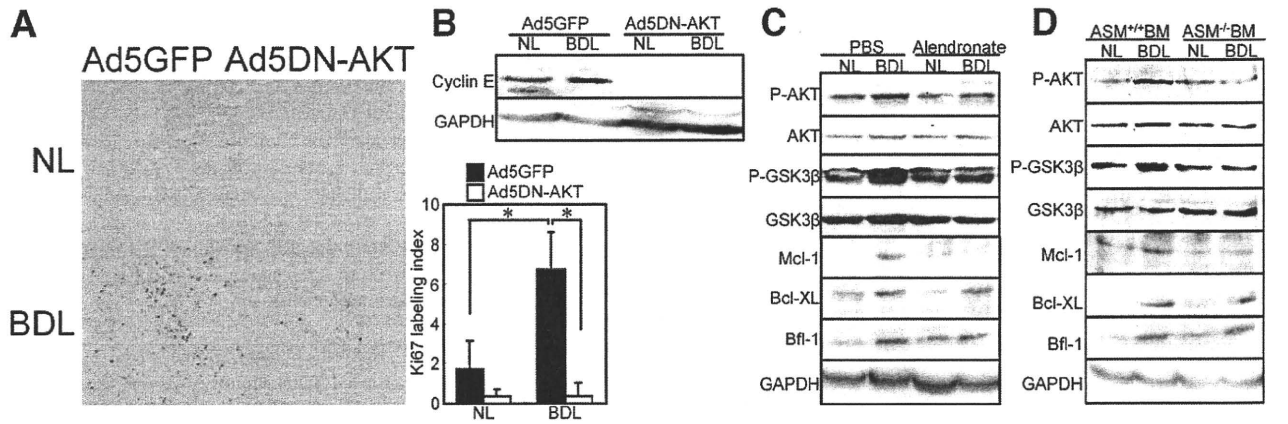

Fig. 7. Kupffer cells and its ASMase are required for AKT activation by BDL. Wildtype mice underwent PBDL and were infected with Ad5GFP or Ad5DN-AKT (A,B) or were treated with Ale-lip or PBS-lip (C). The ASMase$^{+/+}$ bone marrow or ASMase$^{-/-}$ bone marrow-transplanted mice were operated on with PBDL (D). The animals were killed 10 days after the surgery. Expression of Ki67 in the NL right (upper panel) and BDL left (lower panel) lobes were examined by immunohistochemistry (A). (Original magnification ×200.) Ki67 indexes were compared (right panel). Data are means ± SD from at least four independent experiments. *$P < 0.05$ using Student's t test. (B-D) The protein extracts from the livers were subjected to SDS-PAGE and immunoblotting was performed with anti-cyclin E, GAPDH, phosphorylated-AKT, AKT, phosphorylated-GSK3β, GSK3β, Mcl-1, Bcl-XL, and Bfl-1 antibodies. The results shown are representative of at least three independent experiments.

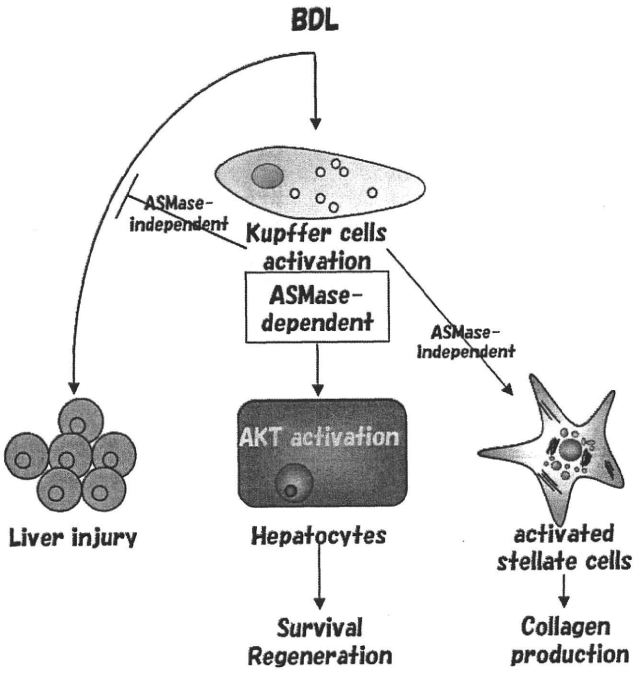

Fig. 8. Hypothetical relations between Kupffer cells and other cells.

ithelial growth factor (HB-EGF), which induce hepatocyte proliferation,[31,32] were not changed in ASMase$^{-/-}$ bone marrow-transplanted mice (Supporting Fig. 7). Accumulation of CD3-positive T cells in BDL lobes in ASMase$^{-/-}$ bone marrow-transplanted mice was also similar to those in ASMase$^{+/+}$ bone marrow-transplanted mice (data not shown). The factors that lead to AKT-dependent hepatocyte protection and regeneration are currently unknown. Further studies are needed to determine these factors.

ASMase has various roles in both parenchymal and nonparenchymal cells. ASMase in hepatocytes modulates hepatocyte apoptosis.[18] Although ASMase in Kupffer cells did not contribute to liver fibrosis, ASMase in HSCs promotes collagen production. Administration of ASMase to human HSCs increased collagen expression. ASMase plus TGF-β treatment further increased collagen production in HSCs (Supporting Fig. 8A). The collagen expression by ASMase is, at least in part, stimulated by way of the modulation of intracellular signals, Smad2/3, downstream targets of TGF-β receptor, and p38, which increases collagen α1(I) mRNA stability in HSCs.[33] The administration of ASMase also phosphorylated p38 (Supporting Fig. 8B). Moreover, exogenous membrane permeable ceramide exerts a stimulatory effect of basal and TGF-β-induced collagen promoter activity in foreskin fibroblast.[34]

In conclusion, Kupffer cells regulate liver injury, hepatocyte survival, regeneration, and fibrosis after chronic liver damage by BDL. AKT activation in hepatocytes, which is induced by way of ASMase of Kupffer cells, is required for the survival and regeneration of hepatocytes. The hypothetical roles of Kupffer cells are schematically summarized in Fig. 8.

References

1. Hirose M, Nishikawa M, Qian W, Haque A, Mashimo M, Inoue M. Mannose-conjugated alendronate selectively depletes Kupffer cells and inhibits endotoxemic shock in the mice. Hepatol Res 2006;36:3-10.
2. Kresse M, Latta M, Kunstle G, Riehle HM, van Rooijen N, Hentze H, et al. Kupffer cell-expressed membrane-bound TNF mediates melphalan hepatotoxicity via activation of both TNF receptors. J Immunol 2005;175:4076-4083.
3. He Q, Kim J, Sharma RP. Fumonisin B1 hepatotoxicity in mice is attenuated by depletion of Kupffer cells by gadolinium chloride. Toxicology 2005;207:137-147.
4. Prins HA, Meijer C, Boelens PG, Diks J, Holtz R, Masson S, et al. Kupffer cell-depleted rats have a diminished acute-phase response following major liver resection. Shock 2004;21:561-565.
5. Ju C, Reilly TP, Bourdi M, Radonovich MF, Brady JN, George JW, et al. Protective role of Kupffer cells in acetaminophen-induced hepatic injury in mice. Chem Res Toxicol 2002;15:1504-1513.
6. Roberts RA, Ganey PE, Ju C, Kamendulis LM, Rusyn I, Klaunig JE. Role of the Kupffer cell in mediating hepatic toxicity and carcinogenesis. Toxicol Sci 2007;96:2-15.
7. Tacke F, Luedde T, Trautwein C. Inflammatory pathways in liver homeostasis and liver injury. Clin Rev Allergy Immunol 2009;36:4-12.
8. Nagata K, Suzuki H, Sakaguchi S. Common pathogenic mechanism in development progression of liver injury caused by non-alcoholic or alcoholic steatohepatitis. J Toxicol Sci 2007;32:453-468.
9. Canbay A, Feldstein AE, Higuchi H, Werneburg N, Grambihler A, Bronk SF, et al. Kupffer cell engulfment of apoptotic bodies stimulates death ligand and cytokine expression. HEPATOLOGY 2003;38:1188-1198.
10. Gehring S, Dickson EM, San Martin ME, van Rooijen N, Papa EF, Harty MW, et al. Kupffer cells abrogate cholestatic liver injury in mice. Gastroenterology 2006;130:810-822.
11. Seki E, De Minicis S, Osterreicher CH, Kluwe J, Osawa Y, Brenner DA, et al. TLR4 enhances TGF-beta signaling and hepatic fibrosis. Nat Med 2007;13:1324-1332.
12. Hannun YA. Functions of ceramide in coordinating cellular responses to stress. Science 1996;274:1855-1859.
13. Bollinger CR, Teichgraber V, Gulbins E. Ceramide-enriched membrane domains. Biochim Biophys Acta 2005;1746:284-294.
14. Sakata A, Ochiai T, Shimeno H, Hikishima S, Yokomatsu T, Shibuya S, et al. Acid sphingomyelinase inhibition suppresses lipopolysaccharide-mediated release of inflammatory cytokines from macrophages and protects against disease pathology in dextran sulphate sodium-induced colitis in mice. Immunology 2007;122:54-64.
15. Dhami R, He X, Gordon RE, Schuchman EH. Analysis of the lung pathology and alveolar macrophage function in the acid sphingomyelinase—deficient mouse model of Niemann-Pick disease. Lab Invest 2001;81:987-999.
16. Utermohlen O, Karow U, Lohler J, Kronke M. Severe impairment in early host defense against Listeria monocytogenes in mice deficient in acid sphingomyelinase. J Immunol 2003;170:2621-2628.
17. Garcia-Ruiz C, Colell A, Mari M, Morales A, Calvo M, Enrich C, et al. Defective TNF-alpha-mediated hepatocellular apoptosis and liver damage in acidic sphingomyelinase knockout mice. J Clin Invest 2003;111:197-208.
18. Osawa Y, Uchinami H, Bielawski J, Schwabe RF, Hannun YA, Brenner DA. Roles for C16-ceramide and sphingosine 1-phosphate in regulating hepatocyte apoptosis in response to tumor necrosis factor-alpha. J Biol Chem 2005;280:27879-27887.